Analysis of the anomalous diffusion in comb structure with absorbing boundary conditions

Lin Liu[a,b], Siyu Chen[a], Libo Feng[c], Jihong Wang[d], Sen Zhang[a], Yanping Chen[a], Xinhui Si[a], Liancun Zheng[a]

[a]*Mathematics and Physics, University of Science and Technology Beijing, Beijing 100083, China*
[b]*State key laboratory of advanced metallurgy, University of Science and Technology Beijing, Beijing 100083, China*
[c]*School of Mathematical Sciences, Queensland University of Technology, GPO Box 2434, Brisbane, QLD. 4001, Australia*
[d]*Beijing Computational Science Research Center, Beijing 100193, P.R. China*

Abstract

The diffusion in comb structure is an important kind of anomalous diffusion with widespread applications. The special structure corresponds to a novel characteristic of anomalous diffusion, which is characterised by the Dirac delta function in the governing equation. By considering the memory characteristic, the fractional derivative is introduced into the constitutive relation, and a new fractional governing equation in the infinite regions is constructed. Instead of simply truncating for the infinite regions, the exact absorbing boundary conditions are deduced by using the (inverse) Laplace transform technique and the stability is analysed. To deal with the governing equation containing the Dirac function, the finite difference method is proposed and the term with the Dirac function is handled using an integration method. The stability and convergence of the numerical scheme are discussed in detail. A fast algorithm is presented that the normal $L1$-scheme is approximated via a sum-of-exponentials approximation. Three examples are conducted, in which the particle distributions and the mean square displacement for the anomalous diffusion in comb structure are discussed. The computational time between the normal numerical scheme and the fast numerical scheme are compared and the rationality and validity of absorbing boundary conditions are analysed. An important finding is that the distribution of the mean square displacement with the absorbing boundary conditions can match the exact one accurately, which demonstrates the effectiveness of the method.

Keywords: Anomalous Diffusion, Fractional Derivative, Fast Algorithm, Absorbing Boundary Conditions, Comb Structure

1. Introduction

Comb structure is named derived from the combs used in our everyday life. As Fig.1.1(a) shows, the comb structure contains a backbone located on the x axis and several teeth which are perpendicular to the backbone. The anomalous diffusion in comb structure has widespread applications, such as the transport of cancer cells [1], the transport along spiny dendrites [2, 3] (see Fig.1.1(b)), the reaction front propagation of actin polymerization [4]. Therefore studying the anomalous diffusion in comb structure has great significance. Due to the special structure, the novel characteristic of the diffusion is that the transport along the x direction only happens along the x axis while the transport along the y direction is normal. For describing the anomalous diffusion behavior, it yields the Fick's constitutive relation [5] containing a special diffusion coefficient with the Dirac delta function along x direction, which is given as

$$J = \left(-D_x \delta(y) \frac{\partial u(x,y,t)}{\partial x} - D_y \frac{\partial u(x,y,t)}{\partial y} \right), \tag{1.1}$$

where J is the diffusion flux, $u(x,y,t)$ is the particle density at the location (x,y) and time t, $D_x\delta(y)$ refers to the diffusion coefficient along the x direction and D_y denotes the diffusion coefficient along the y direction, $\delta(y)$ denotes to the Dirac delta function to reflect the special characteristics of anomalous diffusion along the x direction.

With the further development of research, it is found that Fick's model corresponds to a paradox with an infinite propagation speed [6]. By a modification, considering that the fractional derivative in time reflects the memory characteristic of the transport process [7], yields the following time fractional Fick's constitutive relation [8]

$$J = {}_0^{RL}D_t^{1-\alpha} \left(-D_x \delta(y) \frac{\partial u(x,y,t)}{\partial x}, -D_y \frac{\partial u(x,y,t)}{\partial y} \right), \tag{1.2}$$

(a) (b)

Figure 1.1: (a) The schematic diagram of comb structure. (b) Electron tomogram of a spiny dendrite, which is taken from the website http://www.cacr.caltech.edu/projects/ldviz/results/levelsets/, accessed on 1 July 2013

where the operator ${}_0^{RL}D_t^{1-\alpha}$ refers to the fractional derivative of order $1-\alpha$ based on the Riemann-Liouville definition [9], given as

$$ {}_0^{RL}D_t^{\alpha} g(t) = \frac{1}{\Gamma(1-\alpha)} \frac{d}{dt} \int_0^t \frac{g(\xi)}{(t-\xi)^{\alpha}} d\xi. $$

Combining Eq.(1.2) with the following mass conservation equation

$$ \frac{\partial u(x,y,t)}{\partial t} = -divJ + f_1(x,y,t), \tag{1.3} $$

we obtain the two-dimensional (2D) time fractional governing equation for describing the anomalous diffusion in comb structure, in which the Riemann-Liouville fractional derivative is transferred to a Caputo fractional derivative (the derivation process is given in Appendix A)

$$ {}_0^{C}D_t^{\alpha} u(x,y,t) - D_x \delta(y) \frac{\partial^2 u(x,y,t)}{\partial x^2} - D_y \frac{\partial^2 u(x,y,t)}{\partial y^2} = f(x,y,t), \ t \in (0,T], \ x,y \in \mathbb{R}, \tag{1.4} $$

where $f(x,y,t) = {}_0^{RL}I_t^{1-\alpha} f_1(x,y,t)$ is the source term reflecting the proliferation of particles, the operator ${}_0^{C}D_t^{\alpha}$ refers to the Caputo fractional derivative of order α $(0 < \alpha < 1)$, given as

$$ {}_0^{C}D_t^{\alpha} g(t) = \frac{1}{\Gamma(1-\alpha)} \int_0^t \frac{g'(\xi)}{(t-\xi)^{\alpha}} d\xi. $$

For the sake of simplicity, we introduce the dimensionless quantities

$$ t \to \left(\frac{D_x^2}{D_y^3}\right)^{1/\alpha} t^*, \ x \to \frac{D_x}{D_y} x^*, \ y \to \frac{D_x}{D_y} y^*, \ u \to \frac{D_y^2}{D_x} u^*, \ f \to \frac{D_y^5}{D_x^3} f^*, \ u_0 \to \frac{D_y^2}{D_x} u_0^*, $$

then we have the dimensionless governing equation (the superscript $*$ is omitted for simplicity)

$$ {}_0^{C}D_t^{\alpha} u(x,y,t) - \delta(y) \frac{\partial^2 u(x,y,t)}{\partial x^2} - \frac{\partial^2 u(x,y,t)}{\partial y^2} = f(x,y,t), \ t > 0, \ x,y \in \mathbb{R}, \tag{1.5} $$

with the initial condition

$$ u(x,y,0) = u_0(x,y), \ x,y \in \mathbb{R}, \tag{1.6} $$

and the boundary conditions

$$ u(x,y,t) \to 0, \ \text{when } |x| \to \infty, \ |y| \to \infty \text{ and } t \in (0,T]. \tag{1.7} $$

It is worth mentioning that the anomalous diffusion in the comb model corresponds to the zero boundaries at the infinite regions. The traditional methods to deal with the infinite boundaries are generally truncated by large values with the disadvantage that it goes against the reality that the particle concentration of exterior domains is not zero with time increases, and in turn, the direct truncation also affects the distribution of particle concentration for large

times. Although we can choose a large enough interval to approximate the infinite boundary, it will undoubtedly increase the time in the process of dividing the mesh. How to deal with the zero boundary conditions at the infinite region is of vital importance. In recent works, Gao and Sun [10] applied the finite difference approximation for a class of fractional sub-diffusion equations on an unbounded spatial domain, in which the space unbounded domain is reduced to the space bounded domain by the Laplace transform. Brunner et al. [11] derived the absorbing boundary conditions for a time-fractional diffusion-wave equation on a two-dimensional unbounded spatial domain and obtained the solutions by using finite difference approximations. Zhang et al. [12] derived the exact absorbing boundary conditions for the one-dimensional time fractional Korteweg-de Vries equation. For other important references, the readers can refer to [13, 14, 15, 16, 17, 18, 19, 20].

As a kind of classical and widespread numerical method, the finite difference method is applied to obtain the numerical solution. For solving the governing equation (1.5), one major problem is that the Dirac function exists in the governing equation. To deal with the singular function, a technique to integrate the equation within a finite volume is used that the Dirac function disappears with the help of the integration property. The advantage of this method is that it can eliminate the influence of the singular Dirac function and the error caused by approximating the Dirac function. Based on this numerical scheme, the stability and convergence are analysed in detail.

Due to the non-locality of the time fractional operator, the numerical solution at a certain time depends on all the past discrete time layers by using $L1$-scheme, resulting in a large amount of demand for discrete storage and computation. To build a fast algorithm with flexibility, efficiency and accuracy to reduce the computational cost and save storage is also a problem we are looking forward to solving. In this paper, by referring to the theoretical construct of the fast algorithm in Ref. [21], the nonlocal fractional derivative in the $L1$-scheme is evaluated via a sum-of-exponentials approximation for the convolution kernel. Here we describe the main idea. For the definition of the Caputo's derivative, the integral from 0 to t_n is separated by two parts, $[0, t_{n-1}]$ and $[t_{n-1}, t_n]$. The integral over $[t_{n-1}, t_n]$ can be calculated with the method of the integration by parts. And the core to deal with convolution kernel $t^{-1-\alpha}$ in the integral from $[0, t_{n-1}]$ is approximated by a sum-of-exponentials. For each spatial point, the convolution with the exponential kernel can be evaluated in $O(1)$ time at each time step via standard recurrence relation or any A-stable ordinary differential equation solver [22, 23, 24, 25, 26, 27]. Compared with the direct $L1$ discretisation, the computational cost with the fast algorithm reduces from $O(N^2)$ to $O(NN_{\text{exp}})$ while the storage cost reduces from $O(N)$ to $O(N_{\text{exp}})$, where N and N_{exp} are the total number of time steps and the exponentials needed in the sum-of-exponentials approximation, respectively. Define M as the total number of discretisation points in space. When the similar sum-of-exponentials approximations are used for the exact absorbing boundary conditions as well, the overall computational cost for our algorithm is $O(MNN_{\text{exp}})$ as compared with $O(MN^2)$ for the direct $L1$ method and the storage requirement of our algorithm is $O(MN_{\text{exp}})$ as compared with $O(MN)$ for direct method, where the value of exponentials N_{exp} depends on the prescribed precision ε, the cutoff time step size τ and the final time T.

At the end of the paper, three examples are presented. The first one is to verify the effectiveness of the finite difference scheme by comparing the fast scheme and the normal scheme. The superiority of the calculation with the fast algorithm is analysed. The second one discusses the difference between the absorbing boundary conditions and zero boundary conditions and the validity and rationality of the models. The last one analyses the particle distribution and mean square displacement on the backbone for the anomalous diffusion in comb structure and the impacts of different dynamic parameters. Based on the mean square displacement, the comparison between the model (1.5) with the exact absorbing boundary conditions and conventional boundary conditions is also presented. In addition, the subdiffusion behavior reflected by the mean square displacement is discussed in detail.

The paper is arranged as follows. The absorbing boundary conditions for the model (1.5) is derived in Section 2 and its stability is given in Section 3. The detailed scheme of the finite difference method to treat the governing equation is demonstrated in Section 4. The analysis of the stability and convergence of the finite difference method is presented in Section 5. By substituting the kernel in the convolution integral with the efficient sum-of-exponentials, Section 6 develops the fast algorithm of the finite difference scheme. Three examples are given in Section 7, which mainly demonstrate the effectiveness of the fast discretisation scheme and the accuracy of the exact absorbing boundary conditions. The conclusions are summarised in Section 8.

2. The derivation of exact absorbing boundary conditions

In this section, the artificial boundary method is applied to construct the exact absorbing boundary conditions for problem (1.5)-(1.7). Firstly, the original infinite domain $\Omega := \{(x, y)| -\infty < x < +\infty, -\infty < y < +\infty\}$ is

truncated by a rectangular region $\Omega_c := \{(x,y)|x_l \le x \le x_r, y_d \le y \le y_u\}$, where x_l, x_r, y_d and y_u are the left, right, lower and upper boundaries of Ω_c. The choices of parameters x_l, x_r, y_d and y_u are determined such that the source term $f(x,y,t)$ and initial data $u_0(x,y)$ are compactly supported in Ω_c. Then the infinite domain can be divided into five parts (see Figure 2.1), the computational domain of interest Ω_c, the unbounded exterior domains of the left-upper Ω_{lu}, right-upper Ω_{ru}, left-down Ω_{ld} and right-down Ω_{rd}, respectively given as

$$\Omega_{lu} := \left\{-\infty < x \le x_l, \frac{y_u+y_d}{2} \le y < +\infty\right\} \cup \left\{-\infty < x \le \frac{x_l+x_r}{2}, y_u \le y < +\infty\right\},$$
$$\Omega_{ru} := \left\{x_r \le x < +\infty, \frac{y_u+y_d}{2} \le y < +\infty\right\} \cup \left\{\frac{x_l+x_r}{2} \le x < +\infty, y_u \le y < +\infty\right\},$$
$$\Omega_{ld} := \left\{-\infty < x \le x_l, -\infty < y \le \frac{y_u+y_d}{2}\right\} \cup \left\{-\infty < x \le \frac{x_l+x_r}{2}, -\infty < y \le y_d\right\},$$
$$\Omega_{rd} := \left\{\frac{x_l+x_r}{2} \le x < +\infty, -\infty < y \le y_d\right\} \cup \left\{x_r \le x < +\infty, -\infty < y \le \frac{y_d+y_u}{2}\right\}.$$

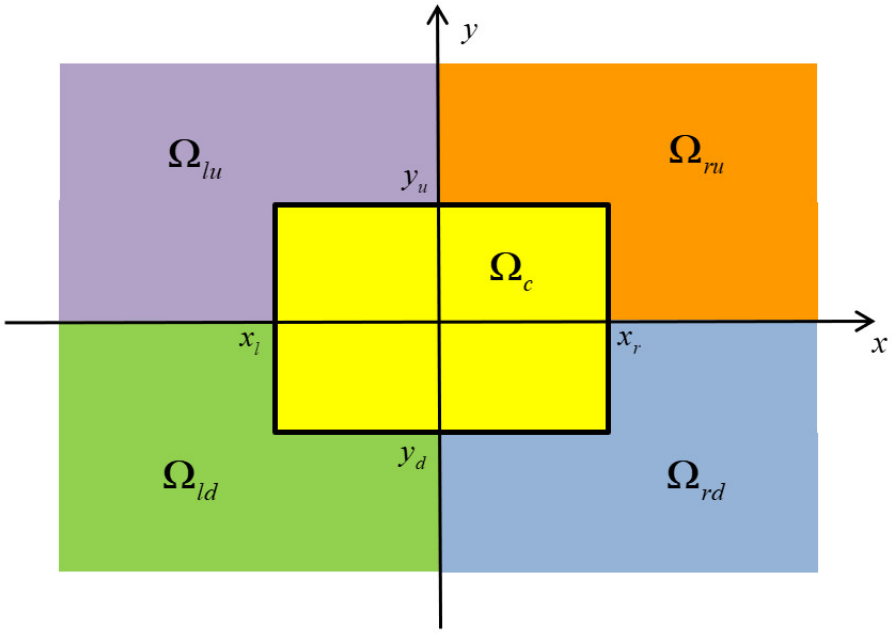

Figure 2.1: The truncated computational domain Ω_c in infinite plane Ω with artificial boundaries $x = x_l$, $x = x_r$, $y = y_d$ and $y = y_u$.

On the four exterior space regions Ω_{lu}, Ω_{ru}, Ω_{ld} and Ω_{rd} and $t > 0$, we have the following governing equation

$$ {}_0^C D_t^\alpha u(x,y,t) - \delta(y)\frac{\partial^2 u(x,y,t)}{\partial x^2} - \frac{\partial^2 u(x,y,t)}{\partial y^2} = 0, \ \ x,y \in \Omega_{lu}, \Omega_{ru}, \Omega_{ld}, \Omega_{rd}, \tag{2.1}$$

subjected to the initial condition

$$u(x,y,0) = 0 \quad \text{for} \quad x,y \in \Omega_{lu}, \Omega_{ru}, \Omega_{ld}, \Omega_{rd}, \tag{2.2}$$

and boundary conditions

$$x,y \in \Omega_{lu} : u(x,y,t) \to 0 \quad \text{when} \quad x \to -\infty, y \to +\infty, \tag{2.3}$$
$$x,y \in \Omega_{ru} : u(x,y,t) \to 0 \quad \text{when} \quad x \to +\infty, y \to +\infty, \tag{2.4}$$
$$x,y \in \Omega_{ld} : u(x,y,t) \to 0 \quad \text{when} \quad x \to -\infty, y \to -\infty, \tag{2.5}$$
$$x,y \in \Omega_{rd} : u(x,y,t) \to 0 \quad \text{when} \quad x \to +\infty, y \to -\infty. \tag{2.6}$$

Performing the Laplace transform [9] on the governing equation (2.1), yields

$$s^{\alpha}\widetilde{u}(x,y,s)-\delta(y)\frac{\partial^2\widetilde{u}(x,y,s)}{\partial x^2}-\frac{\partial^2\widetilde{u}(x,y,s)}{\partial y^2}=0, \tag{2.7}$$

where $\widetilde{u}(x,y,s)=L[u(x,y,t)]$ refers to the Laplace transform of $u(x,y,t)$.

Considering the characteristics of the Dirac delta function, a simplified form $s^{\alpha}\widetilde{u}(x,y,s)-\frac{\partial^2\widetilde{u}(x,y,s)}{\partial y^2}=0$ is formulated for any $y>0$ and $y<0$. According to the characteristic equation $s^{\alpha}-\lambda^2=0$, the eigenvalue is calculated as $\lambda=\pm s^{\alpha/2}$. Then the analytical solution can be expressed as $\widetilde{u}(x,y,s)=c_1(x,s)e^{s^{\alpha/2}y}+c_2(x,s)e^{-s^{\alpha/2}y}$. According to the positive and negative infinite boundary conditions (2.3)-(2.6), we have $\widetilde{u}(x,y,s)=c_2(x,s)e^{-s^{\alpha/2}y}$ for $y>0$ while $\widetilde{u}(x,y,s)=c_1(x,s)e^{s^{\alpha/2}y}$ for $y<0$. Considering the continuity of $\widetilde{u}(x,y,s)$ at $y=0$, we deduce $c_1(x,s)=c_2(x,s)$. Then the solution can be expressed as $\widetilde{u}(x,y,s)=g(x,s)e^{-s^{\alpha/2}|y|}$, where $g(x,s)=c_1(x,s)=c_2(x,s)$. Substituting the solution into Eq.(2.7), we have $\frac{\partial^2 g(x,s)}{\partial x^2}-2s^{\alpha/2}g(x,s)=0$. It is easy to find the solution is $g(x,s)=c_3(s)e^{\sqrt{2}s^{\alpha/4}x}+c_4(s)e^{-\sqrt{2}s^{\alpha/4}x}$. Similarly, using the zero boundary conditions (2.3) at the infinite regions, it yields $g(x,s)=c_4(s)e^{-\sqrt{2}s^{\alpha/4}x}$ for regions Ω_{ru} and Ω_{rd}. Considering the infinite boundary conditions along the x and y directions, it yields

$$\widetilde{u}(x,y,s)=c_4(s)e^{-\sqrt{2}s^{\alpha/4}x}e^{-s^{\alpha/2}y}\text{ for }\Omega_{ru},\quad \widetilde{u}(x,y,s)=c_3(s)e^{\sqrt{2}s^{\alpha/4}x}e^{-s^{\alpha/2}y}\text{ for }\Omega_{lu},$$
$$\widetilde{u}(x,y,s)=c_4(s)e^{-\sqrt{2}s^{\alpha/4}x}e^{s^{\alpha/2}y}\text{ for }\Omega_{rd},\quad \widetilde{u}(x,y,s)=c_3(s)e^{\sqrt{2}s^{\alpha/4}x}e^{s^{\alpha/2}y}\text{ for }\Omega_{ld}.$$

Taking the derivative of the solution with respect to x and y and then performing the inverse Laplace transform, the exact absorbing boundary conditions can be derived as

$$\frac{\partial u(x_l,y,t)}{\partial x}=\sqrt{2}{}_0^C D_t^{\alpha/4}u(x_l,y,t),\quad \frac{\partial u(x_r,y,t)}{\partial x}=-\sqrt{2}{}_0^C D_t^{\alpha/4}u(x_r,y,t), \tag{2.8}$$
$$\frac{\partial u(x,y_u,t)}{\partial y}=-{}_0^C D_t^{\alpha/2}u(x,y_u,t),\quad \frac{\partial u(x,y_d,t)}{\partial y}={}_0^C D_t^{\alpha/2}u(x,y_d,t). \tag{2.9}$$

3. Stability of the model with exact absorbing boundary conditions

We now present the theoretical analysis to verify that the governing equation (1.5) with initial condition (1.6) and boundary conditions (2.8) and (2.9) are stable in L^2-norm. We begin with some useful definitions and lemmas.

Definition 3.1 ([9]). *Suppose a continuous function $g(t)$ is absolutely integrable in $(-\infty,+\infty)$, the Fourier transform is defined as $F_e\{g(t);\omega\}=\hat{G}(\omega)=\int_{-\infty}^{+\infty}e^{-i\omega t}g(t)dt$.*

Lemma 3.1 ([9]). *Suppose a continuous function $g(t)$ is absolutely integrable in $(-\infty,+\infty)$, and the function $g(t)$ satisfies zero initial condition $g(t)\equiv 0$ for $t\le 0$. the Fourier transform for the Caputo fractional derivative is given as $F_e\{{}_0^C D_t^{\alpha}g(t);\omega\}=(-i\omega)^{\alpha}\hat{G}(\omega)$.*

Lemma 3.2 ([28]). *The Plancherel theorem is described as $\int_{-\infty}^{+\infty}|g(t)|^2\,dt=\frac{1}{2\pi}\int_{-\infty}^{+\infty}\left|\hat{G}(\omega)\right|^2 d\omega$.*

Lemma 3.3 ([29]). *Suppose $0<\alpha<1$, it yields $v(t){}_0^C D_t^{\alpha}v(t)\ge\frac{1}{2}{}_0^C D_t^{\alpha}v^2(t)$, where the function $v(t)$ is an absolutely continuous function on $[0,T]$.*

Lemma 3.4 ([9]). *Suppose $a(t)$ and $b(t)$ are nonnegative and nondecreasing and $a(t)$ is locally integrable over $[0,T]$. For $\alpha>0$ and $0\le t\le T$, $v(t)$ satisfies the inequality $v(t)\le a(t)+b(t)\int_0^t(t-\tau)^{\alpha-1}v(\tau)d\tau$, then the following inequality can be deduced $v(t)\le a(t)E_{\alpha}(b(t)\Gamma(\alpha)t^{\alpha})$, where $E_{\alpha}=\sum_{n=0}^{\infty}\frac{z^n}{\Gamma(n\alpha+1)}$ refers to the Mittag-Leffler function.*

Lemma 3.5 ([12]). *Suppose that $y(t)$ is absolutely continuous on $[0,T]$. Then the integral of $y(t)$ satisfies $I_t^1{}_0^C D_t^{\alpha}y(t)=-\frac{t^{1-\alpha}}{\Gamma(2-\alpha)}y(0)+{}_0^{RL}I_t^{1-\alpha}y(t)$, where $I_t^1g(t):=\int_0^t g(s)ds$, the operator ${}_0^{RL}I_t^{1-\alpha}$ refers to the Riemann-Liouville fractional integral of order $1-\alpha$ with the form ${}_0^{RL}I_t^{1-\alpha}g(t)=\frac{1}{\Gamma(1-\alpha)}\int_0^t\frac{g(\xi)}{(t-\xi)^{\alpha}}d\xi$.*

Lemma 3.6. *Supposing f and g are smooth functions, it yields the following inequalities*

$$I_t^1(f_0^C D_t^{\alpha/4} f + g_0^C D_t^{\alpha/4} g)\big|_{t=T} \geq 0, \quad I_t^1(f_0^C D_t^{\alpha/2} f + g_0^C D_t^{\alpha/2} g)\big|_{t=T} \geq 0,$$

where $T > 0$ and $f(0) = g(0) = 0$.

Proof. Firstly, denote $F(t) = f(t)\mathbf{1}_{[0,T]}$ and $G(t) = g(t)\mathbf{1}_{[0,T]}$ for any $T > 0$, where $\mathbf{1}_{0,T}(t)$ is the characteristic function of $[0, T]$ [12]. Then we can extend the integration domain as follows

$$I_t^1(f_0^C D_t^{\alpha/4} f + g_0^C D_t^{\alpha/4} g)\big|_{t=T} = I_t^1(F_0^C D_t^{\alpha/4} F + G_0^C D_t^{\alpha/4} G)\big|_{t=T} = \int_{-\infty}^{+\infty} (F_0^C D_t^{\alpha/4} F + G_0^C D_t^{\alpha/4} G) dt.$$

Employing Lemma 3.1 and the Plancherel theorem in Lemma 3.2, we obtain

$$\begin{aligned}
&\int_{-\infty}^{+\infty} (F_0^C D_t^{\alpha/4} F + G_0^C D_t^{\alpha/4} G) dt = \frac{1}{2\pi} \int_{-\infty}^{+\infty} \left[(-i\omega)^{\alpha/4} \left|\hat{F}(\omega)\right|^2 + (-i\omega)^{\alpha/4} \left|\hat{G}(\omega)\right|^2 \right] d\omega \\
=&\frac{1}{2\pi} \int_{0}^{+\infty} \left[(i\omega)^{\alpha/4} \left|\hat{F}(\omega)\right|^2 + (-i\omega)^{\alpha/4} \left|\hat{F}(\omega)\right|^2 + (i\omega)^{\alpha/4} \left|\hat{G}(\omega)\right|^2 + (-i\omega)^{\alpha/4} \left|\hat{G}(\omega)\right|^2 \right] d\omega \\
=&\frac{1}{2\pi} \cos(\frac{\pi\alpha}{8}) \int_{0}^{+\infty} |\omega|^{\alpha/4} (\left|\hat{F}(\omega)\right|^2 + \left|\hat{G}(\omega)\right|^2) d\omega.
\end{aligned}$$

For $0 < \alpha < 1$, it is easy to conclude that the integral is larger than zero. Following the same process, we can verify the second inequality also holds. □

Lemma 3.7. *For any continuous function $g(y)$, the integral of the product of $g(y)$ and the Dirac function satisfies $\int_{\underline{y}}^{\overline{y}} g(y)\delta(y - y_0)dy = g(y_0)$, where $\underline{y} < y_0 < \overline{y}$.*

Lemma 3.8 ([9])**.** *For any continuous function $g(t)$ and $\alpha, \beta \in \mathbb{R}^+$, it yields ${}_0^{RL}I_t^{\alpha}\, {}_0^{RL}I_t^{\beta} g(t) = {}_0^{RL}I_t^{\alpha+\beta} g(t)$.*

Theorem 3.9. *For $0 < t \leq T$, the governing equation (1.5) with initial condition (1.6) and boundary conditions (2.8) and (2.9) is L^2-stable and satisfy*

$$\int_0^t \|u(\cdot,\cdot,\tau)\|^2 d\tau \leq {}_0^{RL}I_t^{\alpha} \left(\frac{t^{1-\alpha} E_{\alpha}(t^{\alpha})}{\Gamma(2-\alpha)} \right) \|u(\cdot,\cdot,0)\|^2 + {}_0^{RL}I_t^{\alpha} \left(E_{\alpha}(t^{\alpha}) \int_0^t \|f(\cdot,\cdot,\tau)\|^2 d\tau \right), \tag{3.1}$$

where $\|u(\cdot,\cdot,t)\|^2$ is defined as $\|u(\cdot,\cdot,t)\|^2 = \int_{y_d}^{y_u} \int_{x_l}^{x_r} u^2(x,y,t) dxdy$.

Proof. Multiplying both sides of (1.5) with $2u$, integrating x from x_l to x_r, integrating y from y_d to y_u, integrating t over $[0, T]$, and applying the property of the Dirac delta function in Lemma 3.7, we obtain

$$\begin{aligned}
&2\int_0^t \int_{y_d}^{y_u} \int_{x_l}^{x_r} u(x,y,\tau) {}_0^C D_t^{\alpha} u(x,y,\tau) dxdyd\tau - 2\int_0^t \int_{x_l}^{x_r} u(x,0,\tau) \frac{\partial^2 u(x,0,\tau)}{\partial x^2} dxd\tau \\
&-2\int_0^t \int_{y_d}^{y_u} \int_{x_l}^{x_r} u(x,y,\tau) \frac{\partial^2 u(x,y,\tau)}{\partial y^2} dxdyd\tau = 2\int_0^t \int_{y_d}^{y_u} \int_{x_l}^{x_r} f(x,y,\tau) u(x,y,\tau) dxdyd\tau.
\end{aligned} \tag{3.2}$$

For the second term in (3.2), by applying Lemma 3.6, integration by parts and substituting the boundary conditions (2.8), it yields

$$\begin{aligned}
&-2\int_0^t \int_{x_l}^{x_r} u(x,0,\tau) \frac{\partial^2 u(x,0,\tau)}{\partial x^2} dxd\tau = -2\int_0^t \int_{x_l}^{x_r} u(x,0,\tau) d\frac{\partial u(x,0,\tau)}{\partial x} d\tau \\
&= -2\int_0^t \left(u(x,0,\tau) \frac{\partial u(x,0,\tau)}{\partial x} \right) \Big|_{x_l}^{x_r} d\tau + 2\int_0^t \int_{x_l}^{x_r} \frac{\partial u(x,0,\tau)}{\partial x} \frac{\partial u(x,0,\tau)}{\partial x} dxd\tau \\
&= 2\sqrt{2}\int_0^t \left[u(x_r,0,\tau) {}_0^C D_t^{\alpha/4} u(x_r,0,\tau) + u(x_l,0,\tau) {}_0^C D_t^{\alpha/4} u(x_l,0,\tau) \right] d\tau + 2\int_0^t \int_{x_l}^{x_r} \left(\frac{\partial u(x,0,\tau)}{\partial x} \right)^2 dxd\tau \geq 0.
\end{aligned}$$

For the third term in (3.2), by applying Lemma 3.6 and the boundary conditions (2.9), we obtain

$$
\begin{aligned}
&-2\int_0^t\int_{y_d}^{y_u}\int_{x_l}^{x_r} u(x,y,\tau)\frac{\partial^2 u(x,y,\tau)}{\partial y^2}dxdyd\tau = -2\int_0^t\int_{x_l}^{x_r}\int_{y_d}^{y_u} u(x,y,\tau)d\frac{\partial u(x,y,\tau)}{\partial y}dxd\tau\\
&= -2\int_0^t\int_{x_l}^{x_r} u(x,y,\tau)\frac{\partial u(x,y,\tau)}{\partial y}\Big|_{y_d}^{y_u} + 2\int_0^t\int_{x_l}^{x_r}\int_{y_d}^{y_u}\left(\frac{\partial u(x,y,\tau)}{\partial y}\right)^2 dydxd\tau\\
&= -2\int_0^t\int_{x_l}^{x_r}\left[u(x,y_u,\tau)\frac{\partial u(x,y_u,\tau)}{\partial y} - u(x,y_d,\tau)\frac{\partial u(x,y_d,\tau)}{\partial y}\right]dxd\tau + 2\int_0^t\int_{x_l}^{x_r}\int_{y_d}^{y_u}\left(\frac{\partial u(x,y,\tau)}{\partial y}\right)^2 dydxd\tau\\
&= 2\int_0^t\int_{x_l}^{x_r}\left[u(x,y_u,\tau){}_0^C D_t^{\alpha/2}u(x,y_u,\tau) + u(x,y_d,\tau){}_0^C D_t^{\alpha/2}u(x,y_d,\tau)\right]dxd\tau + 2\int_0^t\int_{x_l}^{x_r}\int_{y_d}^{y_u}\left(\frac{\partial u(x,y,\tau)}{\partial y}\right)^2 dydxd\tau \geq 0.
\end{aligned}
$$

We now applying Lemma 3.3 to obtain the simplified form of Eq.(3.2)

$$\int_0^t\int_{y_d}^{y_u}\int_{x_l}^{x_r} {}_0^C D_t^{\alpha} u^2(x,y,\tau)dxdyd\tau \leq 2\int_0^t\int_{y_d}^{y_u}\int_{x_l}^{x_r} f(x,y,\tau)u(x,y,\tau)dxdyd\tau.$$

With the application of Lemma 3.5 and the Cauchy-Schwarz inequality, the above inequality changes as

$$
\begin{aligned}
{}_0^{RL}I_t^{1-\alpha}\int_{y_d}^{y_u}\int_{x_l}^{x_r} u^2(x,y,\tau)dxdy &\leq \frac{t^{1-\alpha}}{\Gamma(2-\alpha)}\int_{y_d}^{y_u}\int_{x_l}^{x_r} u^2(x,y,0)dxdy\\
+\int_0^t\int_{y_d}^{y_u}\int_{x_l}^{x_r} u^2(x,y,\tau)dxdyd\tau &+ \int_0^t\int_{y_d}^{y_u}\int_{x_l}^{x_r} f^2(x,y,\tau)dxdyd\tau. \qquad (3.3)
\end{aligned}
$$

Denote $v(t) := {}_0^{RL}I_t^{1-\alpha}\int_{y_d}^{y_u}\int_{x_l}^{x_r} u^2 dxdy$. Using the property of the Riemann-Liouville integral in Lemma 3.8, we may rewrite $\int_0^t\int_{y_d}^{y_u}\int_{x_l}^{x_r} u^2(x,y,\tau)dxdyd\tau$ as

$$\int_0^t\int_{y_d}^{y_u}\int_{x_l}^{x_r} u^2 dxdyd\tau = {}_0^{RL}I_t^{\alpha}\left({}_0^{RL}I_t^{1-\alpha}\int_{y_d}^{y_u}\int_{x_l}^{x_r}\right) = {}_0^{RL}I_t^{\alpha}v(t).$$

Denote $a(t) := \frac{t^{1-\alpha}}{\Gamma(2-\alpha)}\int_{y_d}^{y_u}\int_{x_l}^{x_r} u^2(x,y,0)dxdy + \int_0^t\int_{y_d}^{y_u}\int_{x_l}^{x_r} f^2(x,y,\tau)dxdyd\tau$ and $b(t) := \frac{1}{\Gamma(\alpha)}$, which satisfy nonnegative and nondecreasing and $a(t)$ is locally integrable over $[0,T]$. Then Eq.(3.3) can be rewritten as

$$v(t) \leq a(t) + {}_0^{RL}I_t^{\alpha}v(t) = a(t) + \frac{1}{\Gamma(\alpha)}\int_0^t (t-\tau)^{\alpha-1}v(\tau)d\tau. \qquad (3.4)$$

A direct application of Lemma 3.4 to (3.4) leads to

$$v(t) \leq a(t)E_{\alpha}(t^{\alpha}). \qquad (3.5)$$

Applying the fractional integral operator ${}_0^{RL}I_t^{\alpha}$ of order α on both sides of (3.5) leads to the desired result (3.1). □

Remark 3.1. *For the special case $u(x,y,0) = \delta(x)\delta(y)$ and $f(x,y,t) = 0$ in model (1.5), the solution to the problem can be expressed as (the detailed deduction is presented in Example 7.3)*

$$u(x,y,t) = \frac{1}{2\sqrt{\pi}}\int_0^{+\infty}\frac{e^{-\frac{x^2}{4\tau}}}{\sqrt{\tau}}L^{-1}\left[s^{\alpha-1}e^{-(2\tau+|y|)s^{\alpha/2}}\right]d\tau, \qquad (3.6)$$

which is difficult to expressed explicitly. However, an important physical characteristics parameter, the mean square displacement, can be derived explicitly as

$$\left\langle \chi^2(t)\right\rangle = \frac{\int_{-\infty}^{+\infty} x^2 u(x,0,t)\,dx}{\int_{-\infty}^{+\infty} u(x,0,t)\,dx} = \Gamma(1-\alpha/2)\,t^{\alpha/2}, \qquad (3.7)$$

which will be used to verify the existence and correctness of the solution.

Theorem 3.10. *Suppose $u(x,y,t)$ and $v(x,y,t)$ are any two solutions of the governing equation (1.5) subjected to the initial condition (1.6) and boundary conditions (2.8) and (2.9), then the two solutions are equal, namely the solution is unique.*

Proof. Suppose $w(x,y,t) = u(x,y,t) - v(x,y,t)$, then $w(x,y,t)$ satisfies the following equation

$$ {}_0^C D_t^\alpha w(x,y,t) - \delta(y)\frac{\partial^2 w(x,y,t)}{\partial x^2} - \frac{\partial^2 w(x,y,t)}{\partial y^2} = 0,\ x,y \in \Omega_c, t > 0, \tag{3.8} $$

subjected to the initial condition

$$ w(x,y,0) = 0 \quad \text{for} \quad x,y \in \Omega_c, \tag{3.9} $$

and the boundary conditions (2.8) and (2.9). A direct application of Theorem 3.9 yields

$$ \int_0^t \|w(\cdot,\cdot,\tau)\|^2 d\tau \le 0. \tag{3.10} $$

Since $\|w(\cdot,\cdot,\tau)\|^2$ is no less than zero, we obtain $w(\cdot,\cdot,\tau) = 0$. The solution has been verified to be unique. □

4. Construction of the finite difference method

In this section, the finite difference method is proposed to solve the time fractional governing equation (1.5) subjected to the initial condition (1.6) and exact absorbing boundary conditions (2.8) and (2.9). For the positive integers N, M_x and M_y, define a uniform temporal partition of time region $[0,T]$ with time steps $\tau = T/N$ and uniform mesh partition of the space region Ω_c with the space steps $h_x = \frac{x_r - x_l}{M_x}$ and $h_y = \frac{y_u - y_d}{M_y}$. Then, we have $t_n = n\tau$ for $n = 0,1,\ldots,N$ and the set of grid points are denoted by $x_i = x_l + ih_x$, $y_j = y_d + jh_y$ for $i = 0,1,\ldots,M_x$ and $j = 0,1,\ldots,M_y$. Besides, denote $u^n = u(\cdot,\cdot,t_n)$, $U_{i,j}^n = u(x_i,y_j,t_n)$ be the exact solution of u at grid points (x_i,y_j,t_n), $u_{i,j}^n$ be the numerical approximation to $u(x_i,y_j,t_n)$ for $i = 0,1,\ldots,M_x$, $j = 0,1,\ldots,M_y$ and $n = 0,1,\ldots,N$. Denote

$$
\begin{aligned}
\delta_x u_{i,j}^n &= \frac{1}{h_x}(u_{i,j}^n - u_{i-1,j}^n), && i = 1,2,\ldots,M_x;\ j = 0,1,\ldots,M_y,\\
\delta_y u_{i,j}^n &= \frac{1}{h_y}(u_{i,j}^n - u_{i,j-1}^n), && i = 0,1,\ldots,M_x;\ j = 1,\ldots,M_y,\\
\delta_x^2 u_{i,j}^n &= \frac{1}{h_x^2}(u_{i+1,j}^n - 2u_{i,j}^n + u_{i-1,j}^n), && i = 1,2,\ldots,M_x-1;\ j = 0,1,\ldots,M_y,\\
\delta_y^2 u_{i,j}^n &= \frac{1}{h_y^2}(u_{i,j+1}^n - 2u_{i,j}^n + u_{i,j-1}^n), && i = 0,1,\ldots,M_x;\ j = 1,2,\ldots,M_y-1.
\end{aligned}
$$

Integrating both sides of the governing equation (1.5) over the finite volume $[y_{j-1/2}, y_{j+1/2}]$ with y, it yields

$$ \int_{y_{j-1/2}}^{y_{j+1/2}} {}_0^C D_t^\alpha u(x,y,t)dy - \int_{y_{j-1/2}}^{y_{j+1/2}} \delta(y)\frac{\partial^2 u(x,y,t)}{\partial x^2}dy - \int_{y_{j-1/2}}^{y_{j+1/2}} \frac{\partial^2 u(x,y,t)}{\partial y^2}dy = \int_{y_{j-1/2}}^{y_{j+1/2}} f(x,y,t)dy. \tag{4.1} $$

According to the rectangle formula, we have

$$
\begin{aligned}
\int_{y_{j-1/2}}^{y_{j+1/2}} {}_0^C D_t^\alpha u(x,y,t)dy &= h_y {}_0^C D_t^\alpha u(x,y_j,t) + O(h_y^3),\\
\int_{y_{j-1/2}}^{y_{j+1/2}} \frac{\partial^2 u(x,y,t)}{\partial y^2}dy &= h_y \frac{\partial^2 u(x,y_j,t)}{\partial y^2} + O(h_y^3),\\
\int_{y_{j-1/2}}^{y_{j+1/2}} f(x,y,t)dy &= h_y f(x,y_j,t) + O(h_y^3).
\end{aligned}
$$

For the simplicity of discussion, suppose M_x and M_y are even and denote $x_{M_x/2}=0$, $y_{M_y/2}=0$, namely, $(x_{M_x/2}, y_{M_y/2})=(0,0)$. Considering the characteristic of the Dirac function, the core to deal with the second term $\delta(y)\frac{\partial^2 u(x,y,t_n)}{\partial x^2}$ is that whether $\delta(y_j)$ is equal to zero. We now apply Lemma 3.7 to obtain

$$\int_{y_{j-1/2}}^{y_{j+1/2}} \delta(y)\frac{\partial^2 u(x,y,t_n)}{\partial x^2}dy = \begin{cases} \frac{\partial^2 u(x,0,t_n)}{\partial x^2}, & \text{for } j=\frac{M_y}{2}, \\ 0, & \text{for } j\neq\frac{M_y}{2}. \end{cases}$$

The singular property of the delta function disappears through the integration of the governing equation. At (x_i, y_j, t_n), the Eq.(4.1) changes as

$${}_0^C D_t^\alpha u(x_i,y_j,t_n) - \frac{1}{h_y}\Phi(y_j)\frac{\partial^2 u(x_i,y_j,t_n)}{\partial x^2} - \frac{\partial^2 u(x_i,y_j,t_n)}{\partial y^2} = f(x_i,y_j,t_n) + O(h_y^2), \tag{4.2}$$

for $0\le i\le M_x,\ 0\le j\le M_y,\ 1\le n\le N$, and $\Phi(y)=\begin{cases} 1, & y=0 \\ 0, & y\neq 0 \end{cases}$.

At $t=t_n$, the $L1$-scheme [30, 31] to approximate the Caputo time fractional derivative of order α $(0<\alpha<1)$ is given as

$${}_0^C D_t^\alpha u^n = \mu\Big[d_0^{(\alpha)}u^n - \sum_{k=1}^{n-1}\big(d_{n-k-1}^{(\alpha)} - d_{n-k}^{(\alpha)}\big)u^k - d_{n-1}^{(\alpha)}u^0\Big] + R_0^{n,\alpha} := D_t^\alpha u^n + R_0^{n,\alpha}, \tag{4.3}$$

where $\mu=\frac{\tau^{-\alpha}}{\Gamma(2-\alpha)}$, $d_0^{(\alpha)}=1$ and $d_k^{(\alpha)}=(k+1)^{1-\alpha}-k^{1-\alpha}$ for $1\le k\le n-1$ and the error $R_0^{n,\alpha}$ satisfies $|R_0^{n,\alpha}|\le C\tau^{2-\alpha}$ when $u^n\in C^2[0,t_n]$.

Using the Taylor expansion, the finite difference discretization for Eq.(4.2) with the initial condition (2.2) and absorbing boundary conditions Eqs.(2.8)-(2.9) is given as

$$D_t^\alpha u_{i,j}^n - \frac{1}{h_y}\Phi(j-M_y/2)\,\delta_x^2 u_{i,j}^n - \delta_y^2 u_{i,j}^n = f_{i,j}^n, \quad 1\le i\le M_x-1,\ 1\le j\le M_y-1,\ 1\le n\le N, \tag{4.4}$$

$$u_{i,j}^0 = u_0(x_i,y_j), \quad 0\le i\le M_x,\ 0\le j\le M_y, \tag{4.5}$$

$$D_t^\alpha u_{0,j}^n - \frac{1}{h_y}\Phi(j-M_y/2)\,\frac{2}{h_x}(\delta_x u_{1,j}^n - \sqrt{2}D_t^{\alpha/4}u_{0,j}^n) - \delta_y^2 u_{0,j}^n = f_{0,j}^n, \quad 1\le j\le M_y-1,\ 1\le n\le N, \tag{4.6}$$

$$D_t^\alpha u_{M_x,j}^n - \frac{1}{h_y}\Phi(j-M_y/2)\,\frac{2}{h_x}(-\sqrt{2}D_t^{\alpha/4}u_{M_x,j}^n - \delta_x u_{M_x,j}^n) - \delta_y^2 u_{M_x,j}^n = f_{M_x,j}^n, \quad 1\le j\le M_y-1,\ 1\le n\le N, \tag{4.7}$$

$$D_t^\alpha u_{i,0}^n - \frac{2}{h_y}(\delta_y u_{i,1}^n - D_t^{\alpha/2}u_{i,0}^n) = f_{i,0}^n, \quad 0\le i\le M_x,\ 1\le n\le N, \tag{4.8}$$

$$D_t^\alpha u_{i,M_y}^n - \frac{2}{h_y}(-D_t^{\alpha/2}u_{i,M_y}^n - \delta_y u_{i,M_y}^n) = f_{i,M_y}^n, \quad 0\le i\le M_x,\ 1\le n\le N. \tag{4.9}$$

In the above, we apply second-order central differences to approximate the spatial derivatives in (4.2) at interior nodes. The discretization for the boundary nodes is based on the following lemma.

Lemma 4.1 ([10]). *Suppose $f(x)\in C^3[x_l,x_r]$, then we have*

$$f''(x_0) - \frac{2}{h_x}\left[\frac{f(x_1)-f(x_0)}{h_x} - f'(x_0)\right] = -\frac{h_x}{3}f^{(3)}(x_0+\theta_1 h_x), \quad \theta_1\in(0,1), \tag{4.10}$$

$$f''(x_{M_x}) - \frac{2}{h_x}\left[f'(x_{M_x}) - \frac{f(x_{M_x})-f(x_{M_x-1})}{h_x}\right] = \frac{h_x}{3}f^{(3)}(x_{M_x}-\theta_2 h_x), \quad \theta_2\in(0,1). \tag{4.11}$$

5. Stability and convergence analysis of the finite difference scheme

In this section, we mainly analyze the stability and convergence of the finite difference scheme (4.4)-(4.9).

Let $\mathbb{V}=\{v|v=(v_{0,0},v_{0,1},\cdots,v_{0,M_y},v_{1,0},v_{1,1},\cdots,v_{1,M_y},\cdots,v_{M_x,0},v_{M_x,1},\cdots,v_{M_x,M_y})\}$. For any $u,v\in\mathbb{V}$, we define the two-dimensional inner product and norm as

$$\begin{aligned}(u,v)_h=\ & \frac{h_x}{2}\left[\frac{h_y}{2}u_{0,0}v_{0,0}+h_y\sum_{j=1}^{M_y-1}u_{0,j}v_{0,j}+\frac{h_y}{2}u_{0,M_y}v_{0,M_y}\right]\\ &+h_x\sum_{i=1}^{M_x-1}\left[\frac{h_y}{2}u_{i,0}v_{i,0}+h_y\sum_{j=1}^{M_y-1}u_{i,j}v_{i,j}+\frac{h_y}{2}u_{i,M_y}v_{i,M_y}\right]\\ &+\frac{h_x}{2}\left[\frac{h_y}{2}u_{M_x,0}v_{M_x,0}+h_y\sum_{j=1}^{M_y-1}u_{M_x,j}v_{M_x,j}+\frac{h_y}{2}u_{M_x,M_y}v_{M_x,M_y}\right],\end{aligned}\tag{5.1}$$

and

$$\|u\|_h=\sqrt{(u,u)_h},\tag{5.2}$$

respectively.

Lemma 5.1. *([15, 30])For any mesh functions $g=\{g^k|0\le k\le N\}$ defined on $\Omega_t=\{t_k|0\le k\le N\}$, the following inequality holds*

$$\tau\sum_{k=1}^{n}(D_t^\alpha g^k)g^k\ge\frac{t_n^{-\alpha}}{2\Gamma(1-\alpha)}\tau\sum_{k=1}^{n}(g^k)^2-\frac{t_n^{1-\alpha}}{2\Gamma(2-\alpha)}(g^0)^2,\quad 1\le n\le N.$$

Theorem 5.2. *For $0<\alpha<1$ and $1\le n\le N$, the finite difference scheme (4.4)-(4.9) is unconditionally stable and it holds*

$$\tau\sum_{n=1}^{N}\|u^n\|_h^2\le\frac{2T}{1-\alpha}\|u^0\|_h^2+4T^{2\alpha}\Gamma(1-\alpha)^2\tau\sum_{n=1}^{N}\|f^n\|_h^2.\tag{5.3}$$

Proof. Performing the inner product between (4.4)-(4.9) with u^n and summing n from 1 to N, yields

$$\tau\sum_{n=1}^{N}\left(D_t^\alpha u^n,u^n\right)_h-\tau\sum_{n=1}^{N}\left(\frac{1}{h_y}\Phi\left(j-M_y/2\right)\delta_x^2u^n,u^n\right)_h-\tau\sum_{n=1}^{N}\left(\delta_y^2u^n,u^n\right)_h=\tau\sum_{n=1}^{N}\left(f^n,u^n\right)_h.\tag{5.4}$$

For the first term of (5.4), applying Lemma 5.1, we have

$$\tau\sum_{n=1}^{N}\left(D_t^\alpha u^n,u^n\right)_h\ge\frac{T^{-\alpha}}{2\Gamma\left(1-\alpha\right)}\tau\sum_{n=1}^{N}\|u^n\|_h^2-\frac{T^{1-\alpha}}{2\Gamma\left(2-\alpha\right)}\|u^0\|_h^2.\tag{5.5}$$

For the second term of (5.4), using the definition of the inner product, we can obtain

$$\begin{aligned}\left(\frac{1}{h_y}\Phi\left(j-M_y/2\right)\delta_x^2u^n,u^n\right)_h=&\left(\delta_xu^n_{1,M_y/2}-\sqrt{2}D_t^{\alpha/4}u^n_{0,M_y/2}\right)u^n_{0,M_y/2}+h_x\sum_{i=1}^{M_x-1}\left(\delta_x^2u^n_{i,M_y/2}\cdot u^n_{i,M_y/2}\right)\\ &+\left(-\sqrt{2}D_t^{\alpha/4}u^n_{M_x,M_y/2}-\delta_xu^n_{M_x,M_y/2}\right)u^n_{M_x,M_y/2}.\end{aligned}\tag{5.6}$$

According to the discrete Green's identity

$$h_x\sum_{i=1}^{M_x-1}\delta_x^2u^n_{i,j}\cdot u^n_{i,j}=-h_x\sum_{i=2}^{M_x-1}\left(\delta_xu^n_{i,j}\right)^2-\delta_xu^n_{1,j}\cdot u^n_{1,j}+\delta_xu^n_{M_x,j}\cdot u^n_{M_x-1,j},\tag{5.7}$$

the Eq.(5.6) can be changed as

$$\begin{aligned}&\left(\frac{1}{h_y}\Phi(j-M_y/2)\delta_x^2u^n,u^n\right)_h\\ =&-h_x\sum_{i=1}^{M_x}\left(\delta_xu^n_{i,M_y/2}\right)^2-\sqrt{2}u^n_{0,M_y/2}D_t^{\alpha/4}u^n_{0,M_y/2}-\sqrt{2}u^n_{M_x,M_y/2}D_t^{\alpha/4}u^n_{M_x,M_y/2}.\end{aligned}\tag{5.8}$$

Similarly, for the third term of (5.4), we have

$$
\begin{aligned}
&\left(\delta_y^2 u^n, u^n\right)_h \\
=&\frac{h_x}{2}\left[\left(\delta_y u_{0,1}^n - D_t^{\alpha/2} u_{0,0}^n\right) u_{0,0}^n + h_y \sum_{j=1}^{M_y-1} \delta_y^2 u_{0,j}^n u_{0,j}^n + \left(-D_t^{\alpha/2} u_{0,M_y}^n - \delta_y u_{0,M_y}^n\right) u_{0,M_y}^n\right] \\
&+ h_x \sum_{i=1}^{M_x-1}\left[\left(\delta_y u_{i,1}^n - D_t^{\alpha/2} u_{i,0}^n\right) u_{i,0}^n + h_y \sum_{j=1}^{M_y-1} \delta_y^2 u_{i,j}^n u_{i,j}^n + \left(-D_t^{\alpha/2} u_{i,M_y}^n - \delta_y u_{i,M_y}^n\right) u_{i,M_y}^n\right] \\
&+ \frac{h_x}{2}\left[\left(\delta_y u_{M_x,1}^n - D_t^{\alpha/2} u_{M_x,0}^n\right) u_{M_x,0}^n + h_y \sum_{j=1}^{M_y-1} \delta_y^2 u_{M_x,j}^n u_{M_x,j}^n + \left(-D_t^{\alpha/2} u_{M_x,M_y}^n - \delta_y u_{M_x,M_y}^n\right) u_{M_x,M_y}^n\right] \\
=&\frac{h_x}{2}\left[-h_y \sum_{j=1}^{M_y}\left(\delta_y u_{0,j}^n\right)^2 - u_{0,0}^n D_t^{\alpha/2} u_{0,0}^n - u_{0,M_y}^n D_t^{\alpha/2} u_{0,M_y}^n\right] \\
&+ h_x \sum_{i=1}^{M_x-1}\left[-h_y \sum_{j=1}^{M_y}\left(\delta_y u_{i,j}^n\right)^2 - u_{i,0}^n D_t^{\alpha/2} u_{i,0}^n - u_{i,M_y}^n D_t^{\alpha/2} u_{i,M_y}^n\right] \\
&+ \frac{h_x}{2}\left[-h_y \sum_{j=1}^{M_y}\left(\delta_y u_{M_x,j}^n\right)^2 - u_{M_x,0}^n D_t^{\alpha/2} u_{M_x,0}^n - u_{M_x,M_y}^n D_t^{\alpha/2} u_{M_x,M_y}^n\right].
\end{aligned} \tag{5.9}
$$

Using the fact that $u_{i,0}^0 = u_{i,M_y}^0 = u_{0,j}^0 = u_{M_x,j}^0 = 0$ by the assumption that the initial data are compactly supported and applying the Lemma 5.1, we obtain

$$
\begin{aligned}
&\tau \sum_{n=1}^{N}\left(u_{0,M_y/2}^n D_t^{\alpha/4} u_{0,M_y/2}^n + u_{M_x,M_y/2}^n D_t^{\alpha/4} u_{M_x,M_y/2}^n\right) \\
\geq&\frac{T^{-\alpha/4}}{2\Gamma(1-\alpha/4)}\tau \sum_{n=1}^{N}\left(u_{0,M_y/2}^n\right)^2 - \frac{T^{1-\alpha/4}}{2\Gamma(2-\alpha/4)}\left(u_{0,M_y/2}^0\right)^2 \\
&+ \frac{T^{-\alpha/4}}{2\Gamma(1-\alpha/4)}\tau \sum_{n=1}^{N}\left(u_{M_x,M_y/2}^n\right)^2 - \frac{T^{1-\alpha/4}}{2\Gamma(2-\alpha/4)}\left(u_{M_x,M_y/2}^0\right)^2 \\
\geq&0.
\end{aligned} \tag{5.10}
$$

Similarly, we derive

$$
\tau \sum_{n=1}^{N}\left(u_{i,0}^n D_t^{\alpha/2} u_{i,0}^n + u_{i,M_y}^n D_t^{\alpha/2} u_{i,M_y}^n\right) \geq 0, \quad 0 \leq i \leq M_x. \tag{5.11}
$$

For the fourth term of (5.4) , we obtain

$$
\tau \sum_{n=1}^{N}\left(f^n, u^n\right)_h \leq \tau \sum_{n=1}^{N}\left(\|f^n\|_h \cdot \|u^n\|_h\right) \leq \tau \sum_{n=1}^{N} T^\alpha \Gamma(1-\alpha)\|f^n\|_h^2 + \tau \sum_{n=1}^{N} \frac{T^{-\alpha}}{4\Gamma(1-\alpha)}\|u^n\|_h^2 \tag{5.12}
$$

$$
\leq T^\alpha \Gamma(1-\alpha)\tau \sum_{n=1}^{N}\|f^n\|_h^2 + \frac{T^{-\alpha}}{4\Gamma(1-\alpha)}\tau \sum_{n=1}^{N}\|u^n\|_h^2. \tag{5.13}
$$

Substituting (5.5)-(5.13) into Eq.(5.4), it derives the following inequality

$$
\frac{T^{-\alpha}}{4\Gamma(1-\alpha)}\tau \sum_{n=1}^{N}\|u^n\|_h^2 \leq \frac{T^{1-\alpha}}{2\Gamma(2-\alpha)}\|u^0\|_h^2 + T^\alpha \Gamma(1-\alpha)\tau \sum_{n=1}^{N}\|f^n\|_h^2. \tag{5.14}
$$

Furthermore, it can be simplified as

$$\tau\sum_{n=1}^{N}\|u^n\|_h^2 \le \frac{2T}{1-\alpha}\|u^0\|_h^2 + 4T^{2\alpha}\Gamma(1-\alpha)^2\tau\sum_{n=1}^{N}\|f^n\|_h^2. \tag{5.15}$$

The proof is completed. □

Now we show the convergence result for the finite difference scheme (4.4)-(4.9).

Theorem 5.3. *Suppose that $u(x,y,t) \in C_{x,y,t}^{4,4,2}(\Omega_c \times [0,T])$ is the solution of problem (1.5) with initial condition (1.6) and boundary conditions (2.8) and (2.9). Denote $U_{i,j}^n = u(x_i, y_j, t_n)$ and $u_{i,j}^n$ be the exact solution and the numerical solution of u at grid points (x_i, y_j, t_n) for $0 \le i \le M_x$, $0 \le j \le M_y$ and $0 \le n \le N$. Define $e_{i,j}^n = U_{i,j}^n - u_{i,j}^n$, then we have the following error estimate*

$$\tau\sum_{n=1}^{N}\|e^n\|_h^2 \le 4T^{2\alpha+1}\Gamma(1-\alpha)^2 C\left(\tau^{4-2\alpha} + \tau^{4-\alpha}/h_y + \tau^{4-\alpha/2}/h_x/h_y + h_x^3/h_y + h_y^3 + h_x h_y^5\right), \tag{5.16}$$

where C is independent of h_x, h_y and τ.

Proof. The error function $e_{i,j}^n$ satisfies the following governing equation:

$$D_t^\alpha e_{i,j}^n - \frac{1}{h_y}\Phi(j - M_y/2)\,\delta_x^2 e_{i,j}^n - \delta_y^2 e_{i,j}^n = R_{i,j}^n, \quad 1 \le i \le M_x - 1,\ 1 \le j \le M_y - 1,\ 1 \le n \le N, \tag{5.17}$$

$$e_{i,j}^0 = 0, \quad 0 \le i \le M_x,\ 0 \le j \le M_y, \tag{5.18}$$

$$D_t^\alpha e_{0,j}^n - \frac{1}{h_y}\Phi(j - M_y/2)\,\frac{2}{h_x}(\delta_x e_{1,j}^n - \sqrt{2}D_t^{\alpha/4} e_{0,j}^n) - \delta_y^2 e_{0,j}^n = R_{0,j}^n, \quad 1 \le j \le M_y - 1,\ 1 \le n \le N, \tag{5.19}$$

$$D_t^\alpha e_{M_x,j}^n - \frac{1}{h_y}\Phi(j - M_y/2)\,\frac{2}{h_x}(-\sqrt{2}D_t^{\alpha/4} e_{M_x,j}^n - \delta_x e_{M_x,j}^n) - \delta_y^2 e_{M_x,j}^n = R_{M_x,j}^n, \quad 1 \le j \le M_y - 1,\ 1 \le n \le N, \tag{5.20}$$

$$D_t^\alpha e_{i,0}^n - \frac{2}{h_y}(\delta_y e_{i,1}^n - D_t^{\alpha/2} e_{i,0}^n) = R_{i,0}^n, \quad 0 \le i \le M_x,\ 1 \le n \le N, \tag{5.21}$$

$$D_t^\alpha e_{i,M_y}^n - \frac{2}{h_y}(-D_t^{\alpha/2} e_{i,M_y}^n - \delta_y e_{i,M_y}^n) = R_{i,M_y}^n, \quad 0 \le i \le M_x,\ 1 \le n \le N. \tag{5.22}$$

By Taylor theorem, it is easy to know that there exists a positive constant C such that (see [10])

$$\begin{aligned}
&|R_{i,j}^n| \le C(\tau^{2-\alpha} + h_y^2), && 0 \le i \le M_x,\ j \ne 0, M_y/2, M_y,\\
&|R_{i,j}^n| \le C(\tau^{2-\alpha} + h_y + \tau^{2-\alpha/2}/h_y), && 0 \le i \le M_x,\ j = 0, M_y,\\
&|R_{i,j}^n| \le C(\tau^{2-\alpha} + h_x^2/h_y + h_y^2), && 1 \le i \le M_x - 1,\ j = M_y/2,\\
&|R_{i,j}^n| \le C(\tau^{2-\alpha} + h_x/h_y + \tau^{2-\alpha/4}/h_x/h_y + h_y^2), && i = 0, M_x,\ j = M_y/2.
\end{aligned} \tag{5.23}$$

According to the Theorem 5.2, we have

$$\begin{aligned}
\tau\sum_{n=1}^{N}\|e^n\|_h^2 &\le \frac{2T}{1-\alpha}\|e^0\|_h^2 + 4T^{2\alpha}\Gamma(1-\alpha)^2\tau\sum_{n=1}^{N}\|R^n\|_h^2\\
&\le 4T^{2\alpha+1}\Gamma(1-\alpha)^2 C\left(\tau^{4-2\alpha} + \tau^{4-\alpha}/h_y + \tau^{4-\alpha/2}/h_x/h_y + h_x^3/h_y + h_y^3 + h_x h_y^5\right).
\end{aligned} \tag{5.24}$$

The proof is completed. □

6. Acceleration of the finite difference scheme

The normal scheme to discretise the time Caputo derivative is the $L1$-scheme, which is very expensive in both the computational and storage cost. This difference scheme contains a summation that involves all history values and the total cost of evaluating the $L1$ discretisation at each point is $O\left(N^2\right)$, where N is the total number of time steps. In order to reduce the computational and storage cost, we now apply a fast algorithm for the evaluation of the Caputo fractional derivative proposed by [21]. Here we present a short summary of the algorithm.

Firstly, the Caputo fractional derivative is divided into two parts, a local part $C_l\left(t_k\right)$ and a history part $C_h\left(t_k\right)$

$$
{}_0^C D_t^\alpha u\left(t\right)|_{t=t_k}=\frac{1}{\Gamma\left(1-\alpha\right)}\int_{t_{k-1}}^{t_k}\frac{u'\left(s\right)ds}{\left(t_k-s\right)^\alpha}+\frac{1}{\Gamma\left(1-\alpha\right)}\int_0^{t_{k-1}}\frac{u'\left(s\right)ds}{\left(t_k-s\right)^\alpha}:=C_l\left(t_k\right)+C_h\left(t_k\right). \tag{6.1}
$$

For dealing with the local part $C_l\left(t_k\right)$, we apply the backward finite difference approximation for $u'(s)$ on the region $[t_{k-1},t_k]$, which yields

$$
C_l\left(t_k\right)\approx\frac{u\left(t_k\right)-u\left(t_{k-1}\right)}{\tau\Gamma\left(1-\alpha\right)}\int_{t_{k-1}}^{t_k}\frac{1}{\left(t_k-s\right)^\alpha}ds=\frac{u\left(t_k\right)-u\left(t_{k-1}\right)}{\tau^\alpha\Gamma\left(2-\alpha\right)}. \tag{6.2}
$$

For the history part $C_h\left(t_k\right)$, we first perform integration by parts to obtain

$$
C_h\left(t_k\right)=\frac{1}{\Gamma\left(1-\alpha\right)}\left[\frac{u\left(t_{k-1}\right)}{\tau^\alpha}-\frac{u\left(t_0\right)}{t_k^\alpha}-\alpha\int_0^{t_{k-1}}\frac{u\left(s\right)ds}{\left(t_k-s\right)^{1+\alpha}}\right]. \tag{6.3}
$$

As [21] shows, the key of the method is that the kernel $\frac{1}{t^{1+\alpha}}$ in the convolution integral can be evaluated by an efficient sum-of-exponentials for any given interval $[\tau,T]$ with a precision ε, such that

$$
\left|\frac{1}{t^{1+\alpha}}-\sum_{l=1}^{N_{\exp}}\omega_l e^{-s_l t}\right|\leq\varepsilon, \tag{6.4}
$$

where s_l and $l=1,2,...,N_{\exp}$ are positive real numbers, t belongs to the region $[\tau,T]$. The number of exponentials $N_{\exp}$ needed is of the order $O\left(\log\frac{1}{\varepsilon}\left(\log\log\frac{1}{\varepsilon}+\log\frac{T}{\tau}\right)+\log\frac{1}{\Delta t}\left(\log\log\frac{1}{\varepsilon}+\log\frac{1}{\tau}\right)\right)$.

For a fixed precision ε, $N_{\exp}=O\left(\log N\right)$ when $T>>1$ and $N_{\exp}=O\left(\log^2 N\right)$ when $T\approx 1$ with $N=\frac{T}{\tau}$. Replacing the convolution kernel $\frac{1}{t^{1+\alpha}}$ in (6.3) by its sum-of-exponentials approximation in (6.4), we obtain

$$
C_h\left(t_k\right)\approx\frac{1}{\Gamma\left(1-\alpha\right)}\left[\frac{u\left(t_{k-1}\right)}{\tau^\alpha}-\frac{u\left(t_0\right)}{t_k^\alpha}-\alpha\sum_{l=1}^{N_{\exp}}\omega_l U_{hist,l}\left(t_k\right)\right], \tag{6.5}
$$

where $U_{hist,l}(t_k)$ satisfies a simple recurrence relation

$$
U_{hist,l}\left(t_k\right)=e^{-s_l\tau}U_{hist,l}\left(t_{k-1}\right)+\int_{t_{k-2}}^{t_{k-1}}e^{-s_l\left(t_k-\tau\right)}u\left(\tau\right)d\tau, \tag{6.6}
$$

with $U_{hist,l}(t_0)=0$ for $l=1,2,\ldots,N_{\exp}$. The integral on the right-hand side of (6.6) can be calculated by a linear approximation of $u(\tau)$ to obtain

$$
\int_{t_{k-2}}^{t_{k-1}}e^{-s_i\left(t_k-\tau\right)}u\left(\tau\right)d\tau\approx\frac{e^{-s_i\tau}}{s_i^2\tau}\left[\left(e^{-s_i\tau}-1+s_i\tau\right)U^{k-1}+\left(1-e^{-s_i\tau}-e^{-s_i\tau}s_i\tau\right)U^{k-2}\right]. \tag{6.7}
$$

By the above recurrence relation, the fast algorithm with the reduction of the computational and storage cost is achieved. As $U_{hist,l}(t_{k-1})$ is already computed and storage, one only needs $O(1)$ cost to compute $U_{hist,l}(t_k)$ at each step. As there are $N_{\exp}$ history nodes altogether, the cost of evaluating the Caputo derivative at each time step changes as $O(N_{\exp})$. That is, the calculated quantity $O(N^2)$ and the storage content $O(N)$ for the direct $L1$-scheme

reduce to $O(\log N)$ or $O(\log^2 N)$ for the given fast scheme, respectively. Substituting (6.2) and (6.5) into (6.1), the fast evaluation of the Caputo fractional derivative can be implemented by the following formula

$$ {}^{F}D_t^{\alpha}u^n := \frac{u^n-u^{n-1}}{\tau^{\alpha}\Gamma(2-\alpha)}+\frac{1}{\Gamma(1-\alpha)}\left[\frac{u^{n-1}}{\tau^{\alpha}}-\frac{u^0}{t_n^{\alpha}}-\alpha\sum_{l=1}^{N_{\exp}}\omega_l U_{hist,l}(t_n)\right], \tag{6.8} $$

where $U_{hist,l}(t_n)$ is evaluated via (6.6) and (6.7). Replacing the L1 discretisation $D_t^{\alpha}u^n$ by its fast version ${}^{F}D_t^{\alpha}u^n$ in the Caputo fractional difference scheme, we obtain an accelerated difference scheme as

$$ {}^{F}D_t^{\alpha}u_{i,j}^n-\frac{1}{h_y}\Phi(j-M_y/2)\,\delta_x^2u_{i,j}^n-\delta_y^2u_{i,j}^n=f_{i,j}^n,\quad 1\le i\le M_x-1,\ 1\le j\le M_y-1,\ 1\le n\le N, \tag{6.9} $$

$$ u_{i,j}^0=u_0(x_i,y_j),\quad 0\le i\le M_x,\ 0\le j\le M_y, \tag{6.10} $$

$$ {}^{F}D_t^{\alpha}u_{0,j}^n-\frac{1}{h_y}\Phi(j-M_y/2)\,\frac{2}{h_x}(\delta_xu_{1,j}^n-\sqrt{2}{}^{F}D_t^{\alpha/4}u_{0,j}^n)-\delta_y^2u_{0,j}^n=f_{0,j}^n,\quad 1\le j\le M_y-1,\ 1\le n\le N, \tag{6.11} $$

$$ {}^{F}D_t^{\alpha}u_{M_x,j}^n-\frac{1}{h_y}\Phi(j-M_y/2)\,\frac{2}{h_x}(-\sqrt{2}{}^{F}D_t^{\alpha/4}u_{M_x,j}^n-\delta_xu_{M_x,j}^n)-\delta_y^2u_{M_x,j}^n=f_{M_x,j}^n,\quad 1\le j\le M_y-1,\ 1\le n\le N, \tag{6.12} $$

$$ {}^{F}D_t^{\alpha}u_{i,0}^n-\frac{2}{h_y}(\delta_yu_{i,1}^n-{}^{F}D_t^{\alpha/2}u_{i,0}^n)=f_{i,0}^n,\quad 0\le i\le M_x,\ 1\le n\le N, \tag{6.13} $$

$$ {}^{F}D_t^{\alpha}u_{i,M_y}^n-\frac{2}{h_y}(-{}^{F}D_t^{\alpha/2}u_{i,M_y}^n-\delta_yu_{i,M_y}^n)=f_{i,M_y}^n,\quad 0\le i\le M_x,\ 1\le n\le N. \tag{6.14} $$

7. Numerical examples

We now report the results of some examples which demonstrate the effectiveness and accuracy of the model with exact absorbing boundary conditions and offer quantitative features of the finite difference scheme in the convergence order and the computational complexity. All the numerical computations were carried out using MATLAB R2015b on a Lenovo desktop with configuration: Intel(R) Xeon(R), Gold 6128 CPU @ 3.40 GHz 3.39 GHz and 256.0 GB RAM. To examine the convergence orders, we define the error norm and convergence order by the formulae

$$ E(h_x,h_y,\tau)=\max_{0\le i\le M_x}\max_{0\le j\le M_j}\left|u(x_i,y_j,t_n)-u_{i,j}^n\right|,\ r_t=\log_2\frac{E(h_x,h_y,\tau)}{E(h_x,h_y,\tau/2)},\ r_s=\log_2\frac{E(h_x,h_y,\tau)}{E(h_x/2,h_y/2,\tau)}. $$

7.1. Example 7.1. Analysis of the max error, convergence order and CPU time

In order to demonstrate the effectiveness of the finite difference scheme, we consider an example with the zero initial value problem. The various source terms reflect different particle proliferation. In our calculation, we set the computational domain $\Omega_c=[-1,1]\times[-1,1]$, final time $T=5$ and the tolerance precision $\varepsilon=10^{-12}$. The exact solution for the problem (1.5) is considered in the form

$$ u(x,y,t)=\begin{cases}(x-1)^2(x+1)^2(y-1)^2(y+1)^2t^2, & x,y\in[-1,1]\times[-1,1],\ t\in[0,T],\\ 0, & x,y\notin[-1,1]\times[-1,1],\ t\in[0,T],\end{cases} $$

which leads to a fixed source term

$$ f(x,y,t)=\begin{cases}(x-1)^2(x+1)^2(y-1)^2(y+1)^2\frac{2t^{2-\alpha}}{\Gamma(3-\alpha)}-4(x-1)^2(x+1)^2\left(3y^2-1\right)t^2\\ -4\left(3x^2-1\right)\delta(y)(y-1)^2(y+1)^2t^2, & x,y\in[-1,1]\times[-1,1],t\in[0,T],\\ 0, & x,y\notin[-1,1]\times[-1,1],t\in[0,T].\end{cases} $$

$h_x = h_y$	Direct time			Fast time			Direct time			Fast time		
	$E(h_x, h_y, \Delta t)$	r_s	CPU(s)	$E(h_x, h_y, \Delta t)$	r_s	CPU(s)	$E(h_x, h_y, \Delta t)$	r_s	CPU(s)	$E(h_x, h_y, \Delta t)$	r_s	CPU(s)
	α=0.2						α=0.4					
1/16	5.5496e-01		4720.50	5.5496e-01		336.88	5.8650e-01		4653.85	5.8650e-01		342.64
1/32	1.3889e-01	2.00	9841.73	1.3889e-01	2.00	417.66	1.4677e-01	2.00	9842.40	1.4677e-01	2.00	424.77
1/64	3.4734e-02	2.00	22939.99	3.4734e-02	2.00	1199.49	3.6701e-02	2.00	23837.03	3.670e-02	2.00	1214.23
1/128	8.6840e-03	2.00	95983.66	8.6840e-03	2.00	4818.13	9.1757e-03	2.00	94281.04	9.1757e-03	2.00	4617.84
1/256	2.1710e-03	2.00	280467.77	2.1710e-03	2.00	18904.21	2.2939e-03	2.00	285024.85	2.2939e-03	2.00	19367.15
	α=0.6						α=0.8					
1/16	6.1819e-01		4292.24	6.1819e-01		347.53	6.4992e-01		4213.81	6.4992e-01		347.82
1/32	1.5467e-01	2.00	9545.92	1.5467e-01	2.00	434.38	1.6259e-01	2.00	9338.82	1.6259e-01	2.00	418.94
1/64	3.8676e-02	2.00	21611.88	3.8676e-02	2.00	1189.63	4.0652e-02	2.00	22812.73	4.0652e-02	2.00	1156.91
1/128	9.6693e-03	2.00	95342.23	9.6693e-03	2.00	5173.93	1.0160e-02	2.00	97616.57	1.0160e-02	2.00	4704.85
1/256	2.4170e-03	2.00	297294.73	2.4170e-03	2.00	17846.56	2.5368e-03	2.00	293049.69	2.5368e-03	2.00	18115.76

Table 7.1: The error, convergence order of $h_x = h_y$ and CPU time for normal and fast schemes with fixed $\tau = 2 \times 10^{-5}$.

τ	Direct time		Fast time		Direct time		Fast time	
	$E(h_x, h_y, \tau)$	r_t	$E(h_x, h_y, \tau)$	r_t	$E(h_x, h_y, \tau)$	r_t	$E(h_x, h_y, \tau)$	r_t
	α=0.2				α=0.4			
1/16	6.02104227e-03		6.0210e-03		1.7817e-02		1.7817e-02	
1/32	1.8367e-03	1.71	1.8367e-03	1.71	6.0576e-03	1.56	6.0576e-03	1.56
1/64	5.5379e-04	1.73	5.5379e-04	1.73	2.0421e-03	1.57	2.0421e-03	1.57
1/128	1.6513e-04	1.75	1.6513e-04	1.75	6.8386e-04	1.58	6.8386e-04	1.58
1/256	4.8474e-05	1.77	4.8474e-05	1.77	2.2753e-04	1.59	2.2753e-04	1.59
	α=0.6				α=0.8			
1/16	4.0632e-02		4.0632e-02		8.32362422e-02		8.32362422e-02	
1/32	1.5631e-02	1.38	1.5631e-02	1.38	3.6544e-02	1.19	3.6544e-02	1.19
1/64	5.9784e-03	1.39	5.9784e-03	1.39	1.5979e-02	1.19	1.5979e-02	1.19
1/128	2.2781e-03	1.39	2.2781e-03	1.39	6.9718e-03	1.20	6.9718e-03	1.20
1/256	8.65640702e-04	1.40	8.6564e-04	1.40	3.0378e-03	1.20	3.0378e-03	1.20

Table 7.2: The error, convergence order of τ and CPU time for normal and fast schemes with fixed $h_x = h_y = 1/5000$.

Tables 7.1 and 7.2 provide a detailed comparison of the errors $E(h_x, h_y, \tau)$ between the exact solution and the numerical solution, the convergence order in time and space and the CPU time between the fast algorithm and the direct method. As can be seen from Table 7.1 and Table 7.2, we find the convergence rate in space is $O(h_x^2 + h_y^2)$ while in time is $O(\tau^{2-\alpha})$. As Eq. (5.16) indicates, the convergence results shown in Theorem 5.3 may not be an optimal order of convergence. Further analysis is our next goal. In addition, from Table 7.1, we have been able to understand the superiority of our fast algorithm when N is large. We can use the fast evaluation to obtain almost the same accuracy as the direct method. As can be reflected from the CPU time in Table 7.1, the fast scheme is much faster than the direct scheme and saves the computational memory for long time simulation. Moreover, we set $M = 128$, $N = 5000$, $\alpha = 0.8$ and the comparison between the numerical solution and the exact solution is shown in Fig.7.1. The distribution of particle concentration shows a bell-shaped surface. As Fig.7.2 shows, the magnitude of the distribution of the error is very small, which indicates that the numerical solution and the exact solution fit very well.

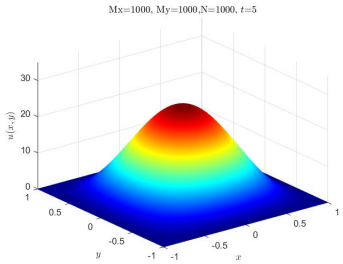

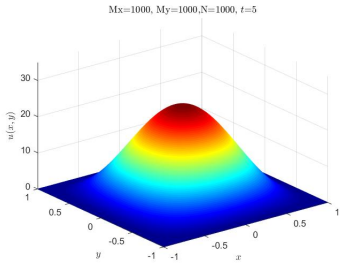

Figure 7.1: The comparison between the exact solution (left) and the numerical solution (right) when $\alpha = 0.5$ and $t = 5$.

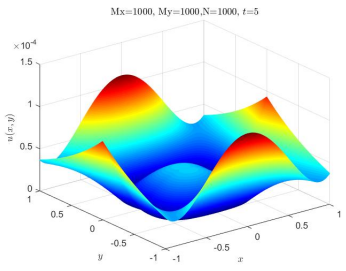

Figure 7.2: The profile of the spatial error between the numerical solution and the exact solution when $\alpha = 0.5$ and $t = 5$.

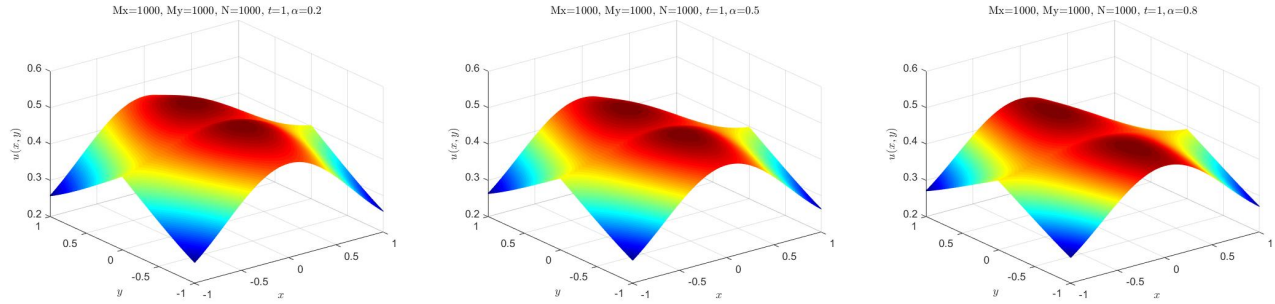

Figure 7.3: The particle distribution for different α at $t = 1$ with the absorbing boundary conditions.

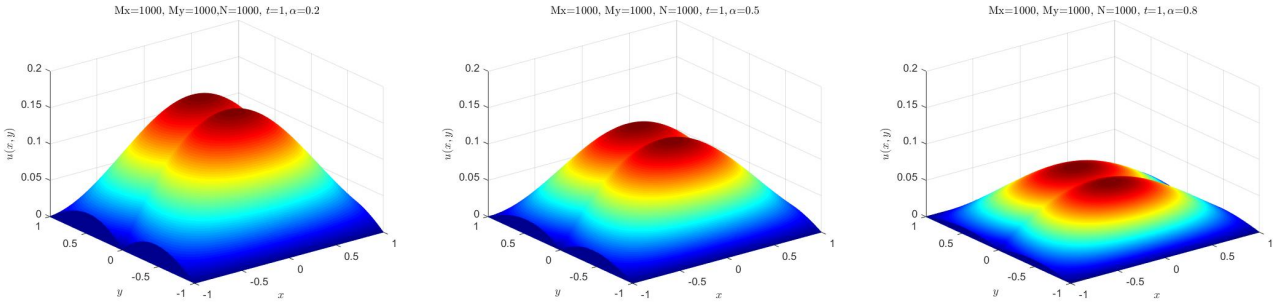

Figure 7.4: The particle distribution for different α at $t = 1$ with the zero boundary conditions.

7.2. Example 7.2. Anomalous diffusion in comb structure with different parameters

In this example, we consider the case $f(x, y, t) = 0$ without considering the particle proliferation. We set the computational domain $\Omega_c = [-1, 1] \times [-1, 1]$ and the tolerance precision $\varepsilon = 10^{-12}$. The initial distribution is $u(x, y, 0) = e^{-x^2-y^2}$. Then we mainly discuss the impacts of different parameters on the particle distribution.

Fig.7.3 gives the three-dimensional particle distribution for the model (1.5) with the absorbing boundary conditions at $t = 1$ for $\alpha = 0.2$, $\alpha = 0.5$, $\alpha = 0.8$, respectively. We can see the impact of α on the particle distribution is mild. A gap at $y = 0$ along the x direction appears due to the fact that the diffusion along the x direction only happens on the backbone. Fig.7.4 presents the particle distribution for the model (1.5) with the zero boundary conditions. Compared with Fig.7.3, the differences of the distribution are that the magnitude of the distribution at the boundary is zero and the impact of α on the particle distribution is significant. Besides, it can be concluded from the global distribution that the zero boundary conditions at the infinite positions not only influences the distribution at the truncated position, but also the overall particle distribution. Thus, the diffusion mechanism cannot be analyzed accurately by the distribution of particles with zero boundary conditions. Finding the absorbing boundary conditions for the model (1.5) in Section 2 is a reasonable and effective method. In addition, the treatment of the problem is to increase the boundary intervals and choose a fine grid size, in this case, takes a long time to compute and cannot simulate the behavior of particle evolution accurately. Fig.7.5 describes the spatial evolution of the particle distribution with increasing time along $y = 0$. The larger the time parameter is, the smaller the magnitude of the distribution at the fixed position is, which describes the transport process of particles from high concentration to low concentration well. Fig.7.6 shows the impacts of different fractional parameters on the particle distribution along $y = 0$. The larger the fractional parameter is, the faster the particles diffuse.

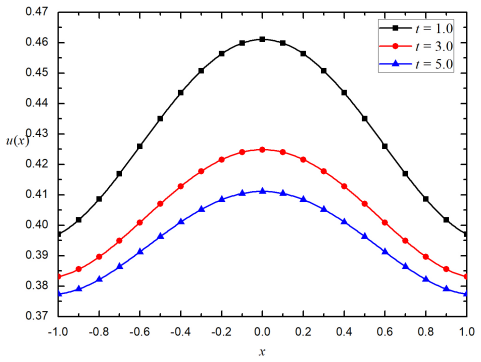

Figure 7.5: The particle distribution versus x at different times for fixed $\alpha = 0.5$ and $y = 0$.

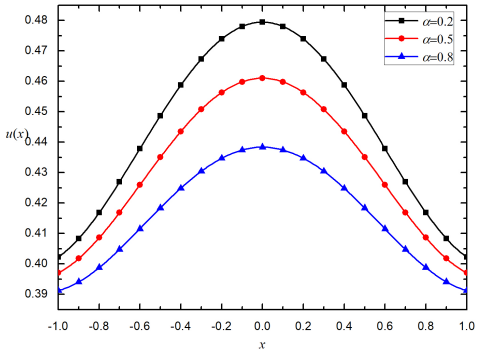

Figure 7.6: The particle distribution versus x with different fractional parameters α for fixed $y = 0$ at $t = 3$.

7.3. Example 7.3. Discussion of the advantage for the model with absorbing boundary conditions

Tracking the particle to find the distribution at any position and time and discussing the mean square displacement are important to analyse the diffusion process in the comb model. This example mainly demonstrates the impacts of the involved parameters on the particle distribution and discusses the superiority of the exact absorbing boundary conditions by comparing them with the exact expression of the mean square displacement. According to the general relationship between the mean square displacement and time $\langle \chi^2(t) \rangle \sim t^\gamma$, the types of anomalous diffusion can be divided into subdiffusion for $0 < \gamma < 1$, superdiffusion for $1 < \gamma < 2$ and the normal diffusion for $\gamma = 1$.

In this example, we consider the initial condition with the form $u(x, y, 0) = \delta(x)\delta(y)$ for problem (1.5). Then the exact mean square displacement can be obtained for the case $f(x, y, t) = 0$ and $u(x, y, t) \to 0$, $|x| \to \infty$, $|y| \to \infty$. Now we present the derivation. Firstly, performing the Laplace transform for time in Eq.(1.5) yields

$$s^\alpha \bar{u}(x, y, s) - s^{\alpha-1}\delta(x)\delta(y) - \delta(y)\frac{\partial^2 \bar{u}(x, y, s)}{\partial x^2} - \frac{\partial^2 \bar{u}(x, y, s)}{\partial y^2} = 0.$$

Imposing the spatial Fourier transform on x leads to

$$s^\alpha \hat{\bar{u}}(k, y, s) - s^{\alpha-1}\delta(y) + \delta(y)k^2 \hat{\bar{u}}(k, y, s) - \frac{\partial^2 \hat{\bar{u}}(k, y, s)}{\partial y^2} = 0, \tag{7.1}$$

where $\hat{\bar{u}}(k, y, s)$ refers to the Fourier transform of $\bar{u}(x, y, s)$. Applying the separate variable method, we define $\hat{\bar{u}}(k, y, s) = h(s, k)e^{-\lambda|y|}$. By using the characteristic of the Dirac delta function, the solution $\hat{\bar{u}}(k, y, s)$ can be obtained as

$$\hat{\bar{u}}(k, y, s) = \frac{s^{\alpha-1}e^{-s^{\alpha/2}|y|}}{2s^{\alpha/2} + k^2} = s^{\alpha-1}e^{-s^{\alpha/2}|y|}\int_0^{+\infty} e^{-2s^{\alpha/2}\tau - k^2\tau}d\tau.$$

Performing the inverse Fourier transform for k to derive

$$\bar{u}(x, y, s) = \frac{s^{\alpha-1}e^{-s^{\alpha/2}|y|}}{2\sqrt{\pi}}\int_0^{+\infty}\frac{1}{\sqrt{\tau}}e^{-2s^{\alpha/2}\tau - \frac{x^2}{4\tau}}d\tau = \frac{1}{2\sqrt{\pi}}\int_0^{+\infty}\frac{e^{-\frac{x^2}{4\tau}}}{\sqrt{\tau}}s^{\alpha-1}e^{-(2\tau+|y|)s^{\alpha/2}}d\tau.$$

Imposing the inverse Laplace transform for s results in

$$u(x, y, t) = \frac{1}{2\sqrt{\pi}}\int_0^{+\infty}\frac{e^{-\frac{x^2}{4\tau}}}{\sqrt{\tau}}L^{-1}\left[s^{\alpha-1}e^{-(2\tau+|y|)s^{\alpha/2}}\right]d\tau. \tag{7.2}$$

Based on (7.2), we can calculate the total number of particles on the backbone

$$\langle u\rangle = \int_{-\infty}^{+\infty} u\left(x,0,t\right)dx = \int_{-\infty}^{+\infty} \frac{1}{2\sqrt{\pi}} \int_{0}^{+\infty} \frac{e^{-\frac{x^2}{4\tau}}}{\sqrt{\tau}} L^{-1}\left[s^{\alpha-1}e^{-2\tau s^{\alpha/2}}\right]d\tau dx = \int_{0}^{+\infty} \frac{\sqrt{4\tau}}{2\sqrt{\tau}} L^{-1}\left[s^{\alpha-1}e^{-2\tau s^{\alpha/2}}\right]d\tau$$
$$= L^{-1}\left(s^{\alpha-1}\int_{0}^{+\infty} e^{-2s^{\alpha/2}\tau}d\tau\right) = L^{-1}\left(s^{\alpha-1}\frac{1}{2s^{\alpha/2}}\right) = \frac{1}{2}L^{-1}\left(s^{\alpha/2-1}\right) = \frac{t^{-\alpha/2}}{2\Gamma\left(1-\alpha/2\right)}.$$

Then we calculate $\left\langle x^2u\right\rangle$

$$\left\langle x^2u\right\rangle = \int_{-\infty}^{+\infty} x^2u\left(x,0,t\right)dx = \int_{-\infty}^{+\infty} x^2\frac{1}{2\sqrt{\pi}} \int_{0}^{+\infty} \frac{e^{-\frac{x^2}{4\tau}}}{\sqrt{\tau}} L^{-1}\left[s^{\alpha-1}e^{-2\tau s^{\alpha/2}}\right]d\tau dx = L^{-1}\left[2s^{\alpha-1}\frac{1}{4s^{\alpha}}\right] = \frac{1}{2}.$$

The exact expression of the mean square displacement can be obtained as

$$\left\langle \chi^2\left(t\right)\right\rangle = \frac{\int_{-\infty}^{+\infty} x^2u\left(x,0,t\right)dx}{\int_{-\infty}^{+\infty} u\left(x,0,t\right)dx} = \Gamma\left(1-\alpha/2\right)t^{\alpha/2}. \tag{7.3}$$

Now, we obtain an important result that the anomalous subdiffusion in the comb model is of order $\alpha/2$ on t.

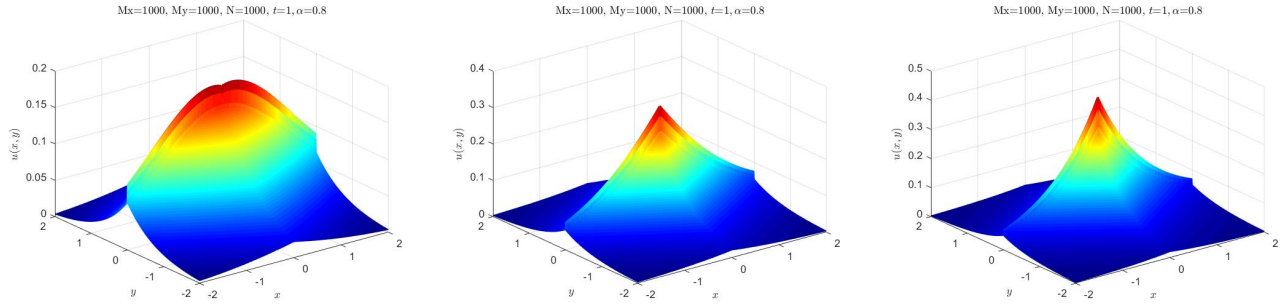

Figure 7.7: The particle distributions of model (1.5) for different α at $t=1$ with the absorbing boundary conditions and $u\left(x,y,0\right)=\delta\left(x\right)\delta\left(y\right)$.

We now compare the model (1.5)-(1.7) with the model (1.5) with the exact absorbing boundary conditions (2.8) and (2.9). Noticing $\delta\left(x\right)$ can be approximated by $\delta\left(x\right)\approx\frac{1}{2\sqrt{\pi\sigma}}\exp\left(-\frac{x^2}{4\sigma}\right)$ with $\sigma\to 0$. In the numerical simulation, we take $\sigma=1\times10^{-4}$ to approximate the Dirac delta function. Fig.7.7 gives the three-dimensional particle distribution for different α that the distribution presents as the bell-shaped forms with a high concentration in the centre position and low concentration at the boundaries. Due to the special structure of the comb structure, the diffusion along the x and y directions are obviously different. The impacts of the fractional parameters α on the particle distribution are significant. In the following, we mainly compute the particle distributions and the mean square displacement on the backbone ($y=0$). Fig.7.8 shows the distribution of the particle concentration at different times. With the increase of time, the distributions decline in the middle and diffuse across the boundaries, which means the particles are moving from high concentration to low concentration. Fig.7.9 shows the impacts of the fractional parameter α on the particle distributions. Time fractional parameter refers to the memory characteristics of the diffusion process. With the increase of fractional parameters, the particle density becomes low at the centre positions and high at the boundaries.

The comparison of the mean square displacement for the model with the exact absorbing boundary conditions, the traditional zero boundary conditions and the exact expression are displayed in Fig.7.10. It is obvious to see the rationality of constructing absorbing boundary conditions that the numerical solution of the model with the exact absorbing boundary conditions agree with the exact solution (7.3) very well, while the distribution with the zero boundary condition deviates the exact solution. In addition, the impacts of different fractional parameters α on the

mean square displacement $\langle \chi^2(t) \rangle$ are shown in Fig.7.11. We can observe that the smaller the fractional parameter is, the slower the particles spread.

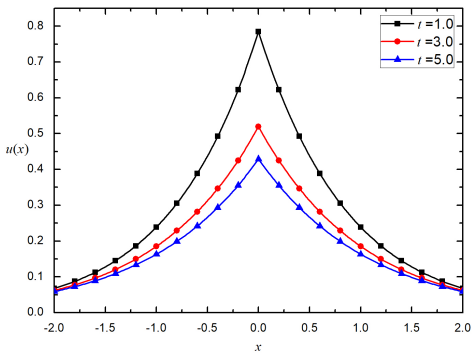

Figure 7.8: The evolution of the particle distribution with time on the backbone for fixed $\alpha = 0.5$.

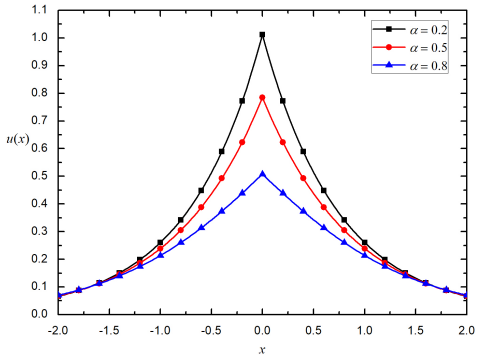

Figure 7.9: The impacts of the fractional parameter on the particle distribution along $y = 0$ at $t = 1$.

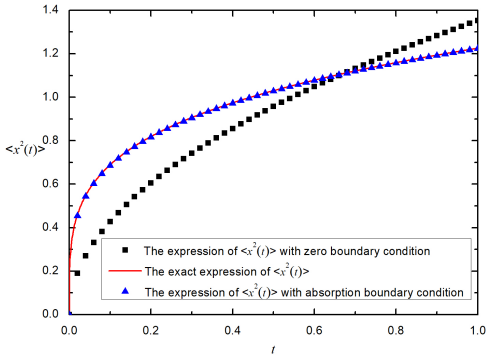

Figure 7.10: The comparison of the mean square displacement for the model with the exact absorbing boundary condition, the traditional zero boundary condition and the exact expression.

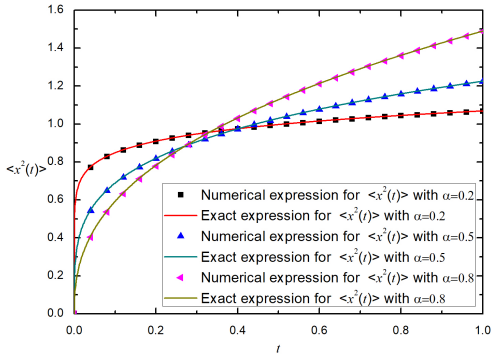

Figure 7.11: The impacts of fractional parameter on the mean square displacement on the backbone.

8. Conclusions

In this paper, based on the background of the anomalous diffusion in comb structure, we constructed the exact absorbing boundary conditions for treating the comb model in the infinite regions and proposed the finite difference method treating the Dirac delta function in the governing equation through an integral over a finite volume. The stability and convergence for the finite difference method were analysed. For more efficient computing, a fast algorithm was proposed. Three examples were presented. One indicated the effectiveness of the finite difference method with the fast scheme, which can greatly reduce the computational cost and save storage without affecting the theoretical accuracy. Another one illustrated the impacts of involved parameters on the particle distribution and discussed the difference in the anomalous diffusion between the absorbing boundary conditions and the zero boundary conditions. The last one analysed the influences of involved parameters on the particle distribution and the mean square displacement on the backbone for the comb model with different boundary conditions. The main results can be summarised as follows:

(1) The absorbing boundary conditions for the comb model on infinite domains is constructed, which is a very useful method for analysing infinite boundary problems;

(2) An efficient finite difference scheme is proposed to solve the model with the exact absorbing boundary conditions, which is stable and convergent. A fast algorithm is developed, which can reduce the computation efficiently without affecting the accuracy;

(3) The validity of the absorbing boundary condition is verified by comparing with the exact solution of the mean square displacement.

(4) Anomalous diffusion in comb model is a kind of subdiffusion problem with the mean square displacement in the form $\left\langle x^2(t)\right\rangle = \Gamma(1-\alpha/2)\, t^{\alpha/2}$.

Acknowledgment

The work is supported by the Project funded by the National Natural Science Foundation of China (No. 11801029), Fundamental Research Funds for the Central Universities (No. FRF-TP-20-013A2)and the Open Fund of State key laboratory of advanced metallurgy in the University of Science and Technology Beijing (N0. K22-08). All the authors wish to thank the anonymous referees for their many constructive comments and suggestions that resulted in an improved version of the paper.

References

[1] A. Iomin, Toy model of fractional transport of cancer cells due to self-entrapping, Phys. Rev. E 73 (6) (2006) 061918.

[2] A. Iomin, V. Méndez, Reaction-subdiffusion front propagation in a comblike model of spiny dendrites, Phys. Rev. E 88(1) (2013) 012706.

[3] V. Méndez, A. Iomin, Comb-like models for transport along spiny dendrites, Chaos Solitons Fractals 53 (2013) 46-51.

[4] A. Iomin, V. Zaburdaev, T. Pfohl, Reaction front propagation of actin polymerization in a comb-reaction system, Chaos Solitons Fractals 92 (2016) 115-122.

[5] J. Crank, The mathematics of diffusion, Oxford, Clarendon, 1970.

[6] C.I. Christov, P.M. Jordan, Heat conduction paradox involving second-sound propagation in moving media, Phys. Rev. Lett. 94 (2015) 154301.

[7] M. Du, Z. Wang, H. Hu, Measuring memory with the order of fractional derivative, Sci. Rep. 3 (2013) 03431.

[8] L. Liu, L. Zheng, F. Liu, X. Zhang, Exact solution and invariant for fractional Cattaneo anomalous diffusion of cells in two dimensional comb framework, Nonlinear Dyn. 89 (2017) 213-224.

[9] I. Podlubny, Fractional differential equation, San Diego: Academic Press, 1999.

[10] G. Gao, Z. Sun, The finite difference approximation for a class of fractional sub-diffusion equations on a space unbounded domain, J. Comput. Phys. 236 (2013) 443-460.

[11] H. Brunner, H. Han, D. Yin, Artificial boundary conditions and finite difference approximations for a time-fractional diffusion-wave equation on a two-dimensional unbounded spatial domain, J. Comput. Phys. 276 (2014) 541-562.

[12] Q. Zhang, J. Zhang, S. Jiang, Z. Zhang, Numerical solution to a linearized time fractional Kdv equation on unbounded domains, Math. Comput. 87 (2018) 693-719.

[13] W. Zhang, H. Li, X. Wu, Local absorbing boundary conditions for a linearized Kortewegde Vries equation, Phys. Rev. E 89 (5) (2014) 053305.

[14] B. Li, J. Zhang, C. Zheng, Stability and error analysis for a second-order fast approximation of the one-dimensional Schrödinger equation under absorbing boundary conditions, SIAM J. Sci. Comput. 40 (2018) 4083-4104.

[15] G. Gao, Z. Sun, Y. Zhang, A finite difference scheme for fractional sub-diffusion equations on an unbounded domain using artificial boundary conditions, J. Comput. Phys. 231 (2012) 2865-2879.

[16] J. Szeftel, A nonlinear approach to absorbing boundary conditions for the semilinear wave equation, Math. Comput. 75 (2006) 565-594.

[17] S. Ji, G. Pang, X. Antoine, J. Zhang, Artificial boundary conditions for the semi-discretized one-dimensional nonlocal Schrödinger equation, J. Comput. Phys. 444 (2021) 110575.

[18] Z. Sun, X. Wu, The stability and convergence of a difference scheme for the Schrödinger equation on an infinite domain by using artificial boundary conditions, J. Comput. Phys. 214 (2006) 209-223.

[19] H. Han, Z. Huang, A class of artificial boundary conditions for heat equation in unbounded domains, Comput. Math. Appl. 43 (2002) 889-900.

[20] X. Antoine, Artificial boundary conditions for one-dimensional cubic nonlinear Schrödinger equations, SIAM J. Sci. Comput. 43 (2006) 2272-2293.

[21] S. Jiang, J. Zhang, Q. Zhang, Z. Zhang, Fast evaluation of the Caputo fractional derivative and its applications to fractional diffusion equations, Commun. Comput. Phys. 21 (2017) 650-678.

[22] B. Alpert, L. Greengard, T. Hagstrom, Rapid evaluation of nonreflecting boundary kernels for time-domain wave propagation, SIAM J. Numer. Anal. 37 (2000) 1138-1164.

[23] B. Alpert, L. Greengard, T. Hagstrom, Nonreflecting boundary conditions for the time-dependent wave equation, J. Comput. Phys. 180 (2002) 270-296.

[24] D. Baffet, J. S. Hesthaven, A Laplace transform based kernel reduction scheme for fractional differential equations, SIAM J. Numer. Anal. 55 (2016) 496-520.

[25] C. Zheng, Approximation, stability and fast evaluation of exact artificial boundary condition for the one-dimensional heat equation, J. Comput. Math. 25 (2007) 730-745.

[26] S. Jiang, Fast evaluation of the nonreflecting boundary conditions for the Schrödinger equation, Ph.D. thesis, Courant Institute of Mathematical Sciences, New York University, New York, 2001.

[27] J.-R. Li, A fast time stepping method for evaluating fractional integrals, SIAM J. Sci. Comput. 31 (2009) 4696-4714.

[28] R. Penney, Abstract Plancherel theorems and a Frobenius reciprocity theorem, J. Func. Anal. 18 (1975) 177-190.

[29] A.A. Alikhanov, A priori estimates for solutions of boundary value problems for equations of fractional order, Differ. Uravn. 46 (2010) 658-664.

[30] Z. Sun, X. Wu, A fully discrete difference scheme for a diffusion-wave system, Appl. Numer. Math. 56 (2006) 193-209.

[31] Y. Lin, C. Xu, Finite difference/spectral approximations for the time-fractional diffusion equation. J. Comput. Phys. 225(2) (2007) 1533-1552.

[32] H. Neudecker, A note on Kronecker products and matrix equation systems, SIAM J. Appl. Math. 17 (1969) 603-606.

Appendix A.

In this section, we present the derivation of (1.4), i.e., the equivalence between the governing equations with the Caputo fractional derivative and the Riemann-Liouville fractional derivative.
The governing equations

$$\frac{\partial u\left(x,y,t\right)}{\partial t}={}_{0}^{RL}D_{t}^{1-\alpha}\frac{\partial^{2}u\left(x,y,t\right)}{\partial x^{2}}+f_{1}\left(x,y,t\right), \tag{8.1}$$

and

$${}_{0}^{C}D_{t}^{\alpha}u\left(x,y,t\right)=\frac{\partial^{2}u\left(x,y,t\right)}{\partial x^{2}}+{}_{0}^{RL}I_{t}^{1-\alpha}f_{1}\left(x,y,t\right), \tag{8.2}$$

are equivalent.
Proof: Performing the RL fractional integral ${}_{0}^{RL}I_{t}^{1-\alpha}$, the left side of Eq. (8.1) equals to

$${}_{0}^{RL}I_{t}^{1-\alpha}\frac{\partial u\left(x,y,t\right)}{\partial t}={}_{0}^{RL}D_{t}^{\alpha}u\left(x,y,t\right)-u\left(x,y,0\right)\frac{t^{-\alpha}}{\Gamma\left(1-\alpha\right)}={}_{0}^{C}D_{t}^{\alpha}u\left(x,y,t\right),$$

and the right side of Eq. (8.1) equals

$$\begin{aligned}&{}_{0}^{RL}I_{t}^{1-\alpha}{}_{0}^{RL}D_{t}^{1-\alpha}\frac{\partial^{2}u\left(x,y,t\right)}{\partial x^{2}}+{}_{0}^{RL}I_{t}^{1-\alpha}f_{1}\left(x,y,t\right)\\&=\frac{\partial^{2}u\left(x,y,t\right)}{\partial x^{2}}-\left[{}_{0}^{RL}I_{t}^{\alpha}\frac{\partial^{2}u\left(x,y,t\right)}{\partial x^{2}}\right]\Big|_{t=0}\frac{t^{-\alpha}}{\Gamma\left(1-\alpha\right)}+{}_{0}^{RL}I_{t}^{1-\alpha}f_{1}\left(x,y,t\right),\end{aligned}$$

where

$$\begin{aligned}&\left[{}_{0}^{RL}I_{t}^{\alpha}\frac{\partial^{2}u\left(x,y,t\right)}{\partial x^{2}}\right]\Big|_{t=0}=\lim_{t\to0}\frac{1}{\Gamma\left(\alpha\right)}\int_{0}^{t}\frac{1}{\left(t-s\right)^{1-\alpha}}\frac{\partial^{2}u\left(x,y,s\right)}{\partial x^{2}}ds\\&=-\lim_{t\to0}\frac{1}{\Gamma\left(1+\alpha\right)}\int_{0}^{t}\frac{\partial^{2}u\left(x,y,s\right)}{\partial x^{2}}d(t-s)^{\alpha}\\&=\lim_{t\to0}\frac{1}{\Gamma\left(1+\alpha\right)}\left[\frac{\partial^{2}u\left(x,y,0\right)}{\partial x^{2}}t^{\alpha}+\int_{0}^{t}\frac{\partial}{\partial t}\left(\frac{\partial^{2}u\left(x,y,s\right)}{\partial x^{2}}\right)\left(t-s\right)^{\alpha}ds\right]=0.\end{aligned}$$

Namely, the two equations (8.1) and (8.2) are equivalent.